

SEMMELWEIS EGYETEM
DOKTORI ISKOLA

Ph.D. értekezések

2949.

REÉ DÓRA

Patobiokémia

című program

Programvezető: Dr. Csala Miklós, egyetemi tanár
Témavezető: Dr. Apáti Ágota, tudományos főmunkatárs

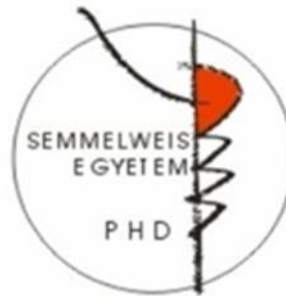
**Establishment and characterization of a DGCR8 monoallelic human
pluripotent stem cell line**

Ph.D. thesis

Dóra Reé

Molecular Medicine Doctoral School

Semmelweis University



Supervisor: Ágota Apáti, Ph.D.

Official reviewers: Karolina Piracs, Ph.D.

Melinda Purity, Ph.D.

Head of the Complex Examination Committee: Miklós Kellermayer, M.D., D.Sc.

Members of the Complex Examination Committee: Attila Tordai, Ph.D., D.Sc.

Elen Góczá, Ph.D., D.Sc.

Budapest

2023

Table of Contents

List of abbreviations.....	2
1. Introduction.....	5
1.1. DiGeorge Syndrome (DGS, 22q11.2DS)	5
1.1.1 <i>DGCR8 (DiGeorge Syndrome Critical Region 8)</i>	5
1.2. miRNAs.....	8
1.2.1 <i>miRNA biogenesis</i>	9
1.2.2 <i>miRNA clusters</i>	12
1.2.3 <i>Posttranscriptional regulation of clustered miRNAs</i>	12
1.3. Human pluripotent stem cells.....	13
1.3.1 <i>Classification of pluripotent stem cells (hPSCs)</i>	14
1.3.2 <i>Characterization of hPSCs</i>	15
1.3.3 <i>Genetic engineering in hPSCs</i>	17
1.3.4 <i>In vitro disease modeling with hPSCs</i>	19
2. Objectives	21
3. Methods.....	22
4. Results	26
4.1. Establishment of the DGCR8 deficient hESC line	26
4.2. Gradual loss of transgene expression in DGCR8 ^{+/-} hESCs.....	29
4.3. Selected single cell clones contain certain regions of the insert.	32
4.4. DGCR8 ^{+/-} hESCs maintain pluripotency and trilineage differentiation capacity.	33
4.5. DGCR8 ^{+/-} hESCs show decreased DGCR8 expression.	36
4.6. DGCR8 ^{+/-} hESCs show partial disturbance of Microprocessor function.....	37
5. Discussion.....	39
6. Conclusions.....	44
7. Summary	46
8. References.....	47
9. Bibliography of the candidate’s publication	67
9.1. Publications related to the PhD thesis.....	67
9.2. Other publications.....	67
10. Acknowledgements	68
Supplementary material	69

List of abbreviations

22q11.2DS - 22q11.2 Deletion Syndrome / DiGeorge Syndrome

Ago – Argonaute protein

AD - Alzheimer's disease

AP – Alkaline phosphatase

ASD - autism spectrum disorder

BMC - bone marrow cell

C19MC - chromosome 19 microRNA cluster

CAG - CMV immediate enhancer/ β -actin

cNCC - cardiac neural crest cell

CNS - central nervous system

CRISPR – clustered regulatory interspaced short palindromic repeats

crRNA - CRISPR RNA

DDX1 - RNA helicase DEAD-Box Helicase 1

DGCR8 – DiGeorge Syndrome Critical Region 8

DGS - DiGeorge Syndrome

DSB - double-strand break

EIF1A - eukaryotic translation initiation factor 1A

ERH - enhancer of rudimentary homolog

ESC – embryonic stem cell

FACS – fluorescence-activated cell sorting

hESC - Human embryonic stem cell

hiPSC- human induced pluripotent stem cell

hiPSC-CM - hiPSC-derived cardiomyocyte

hMSC - human mesenchymal stem cell

HDR - homology-directed repair

hnRNPA1 - heterogeneous nuclear ribonucleoprotein A1

HR - homologous recombination

iPSC – induced pluripotent stem cell

L1 - LINE-1

lincRNA - long intergenic noncoding RNA

mRNA – messenger RNA

miRNA – microRNA

NHEJ - non-homologous end joining

PAM - protospacer-associated motif

PSC – pluripotent stem cell

pre-miRNA - precursor microRNA

pri-miRNA - primary micro RNA

RISC – RNA-induced silencing complex

RNP - ribonucleoprotein

SAFB2 - scaffold Attachment Factor B2

SCID – severe combined immunodeficiency

SCZ - schizophrenia

snoRNA - small nucleolar RNA

shRNA - short hairpin RNA

sgRNA - single guide RNA

t-RNA - transfer RNA

Tbr1 - T-Box Brain Transcription Factor 1

Tcf711 - T-cell factor 3 gene

TALEN – transcription activator-like effector nuclease

tracrRNA - trans-activating CRISPR RNA

XPO5 - Exportin-5

ZNF - zinc finger nuclease

1. Introduction

1.1. DiGeorge Syndrome (DGS, 22q11.2DS)

DiGeorge syndrome is a genetic disorder resulting from the hemizygous deletion of a 1.5-3 Mb segment of chromosome 22 [1,2]. This monoallelic deletion impacts critical genes that play important roles in the development of various organs and systems, including the thymus, parathyroid glands, and heart. Consequently, individuals with DGS often exhibit a wide range of medical problems, including congenital heart disease, palatal abnormalities, gastrointestinal anomalies, immune deficiency, central nervous system (CNS) abnormalities, psychiatric diseases, skeletal anomalies, and hearing loss. The severity of these symptoms can vary widely regardless of the size of the deletion [3–5]. While the cellular function of some candidate genes is well studied, their contribution to the development of diseased phenotypes in individuals with DiGeorge syndrome is yet to be determined. [6,7].

1.1.1 DGCR8 (DiGeorge Syndrome Critical Region 8)

Situated within the 22q11.2 region, DGCR8 (DiGeorge Syndrome Critical Region 8) is among the 30 to 90 affected genes in DGS, with DGCR8 haploinsufficiency representing a prevalent occurrence in the patients [7,8]. Being a complex disorder, the exact role of DGCR8 in the development of DGS is not obvious, but its contribution to the disease is beyond doubt. DGCR8 functions as a subunit of the Microprocessor complex, which is a vital contributor to canonical miRNA biogenesis and therefore, to global gene regulation. Investigations into its functions have unveiled its vital role in the early stages of embryogenesis; studies involving *Dgcr8*^{-/-} mouse embryos have shown its profound impact on embryonic progression, resulting in early arrest in development [9]. To gain deeper insight into the relevance of *Dgcr8* in the context of embryonic stem cell (ESC) differentiation, the Blelloch group generated and characterized ESC lines in 2007 [9]. They found that complete knockout mESCs arrest in G1 phase of the cell cycle and have extended population doubling time. More intriguingly, *Dgcr8*-deficient mESCs demonstrated impaired differentiation primarily attributed to their inability to fully down-regulate pluripotency markers. These defected phenotypes were all suspected to be caused by disturbances in miRNA processing [9]. Given the phenotype of *Dgcr8*^{-/-} ESCs,

studying the exact role of complete deletion of *Dgcr8* in distinct contexts requires conditional or cell type-specific *Dgcr8* knockout models [10]. Inactivation of *Dgcr8* in the cardiac neural crest cells (cNCCs) in mice results in major cardiovascular defects at E18.5 caused by the reduction of the progenitor pool required for outflow tract remodeling [11]. In muscle specific *Dgcr8* knockout mice, the maintenance of mature cardiac muscle is impaired, leading to diluted cardiomyopathy and heart failure [12]. Deletion of *Dgcr8* in *Mesp1* cardiovascular progenitor cells yields an enlarged heart due to defective cardiomyocyte differentiation coupled with unusual upregulation in vascular gene expression [13]. Targeted ablation in early B cell precursors prompt a developmental block at the pro-B cell stage [14]. Intriguingly, *Dgcr8* inactivation in bone marrow cells (BMCs) does not disrupt differentiation to macrophages, but the resulting cells show overshooting expression of *IFN β* and ISG upon mycobacterial infection [15]. Several mouse models have been generated through the deletion of a genomic segment in mice syntenic to the human 22q11.2 locus (*Df16^{+/-}* or *Lgdel^{+/-}*). *Df16^{+/-}* mice typically exhibit core structural and behavioral abnormalities observed in schizophrenia (SCZ), including impaired sensorimotor gating function, learning and memory deficits, abnormalities in the prefrontal cortex and hippocampus with additional signs of miRNA dysregulation [16–18]. *Dgcr8^{+/-}* mice recapitulate a significant, yet not exclusive portion of these phenotypes, often displaying altered neuronal morphology, short- and long-term plasticity and miRNA dysregulation with pri-miRNA enrichment [19–21]. Some of these alterations rather emerge later in development, suggesting defected neuronal maturation [17,20]. To our knowledge, only two studies have been published involving hiPSCs with partial or complete DGCR8 loss. The first studied DGCR8^{-/-} iPSCs, revealing altered cell cycle, poor maintenance, limited self-renewal capacity coupled with spontaneous differentiation [22]. In another study, DGS and DGCR8^{+/-} hiPSCs underwent 2D and 3D cortical neuronal differentiation, exhibiting modified resting potential resulting in calcium signaling defects and irregular spontaneous neuronal activity. Remarkably, DGCR8 overexpression rescued the impaired phenotype in both DGS and DGCR8^{+/-} cells [23]. There is a growing body of evidence for the existence of new, non-canonical functions of Microprocessor components. In 2012 an HITS-Clip analysis conducted by the Cáceres group unveiled, that binding partners of DGCR8 included several hundred mRNAs, as well as snoRNAs and lincRNAs (long intergenic non-coding RNAs) [24].

Furthermore, it was demonstrated that DGCR8 is essential for the recruitment of the exosome to human telomerase RNA and snoRNA thereby regulating snoRNA decay [25]. These findings could elucidate the transcriptional differences in small RNAs between *Dicer*^{-/-} and *Dgcr8*^{-/-} cells [26]. DGCR8 has also been reported to engage with heterochromatin and nuclear lamina proteins in human mesenchymal stem cells (hMSCs) leading to accelerated senescence. Notably, this study highlighted DGCR8's declining levels with aging and showed that lentiviral DGCR8 expression rescued deficits in a mouse model of articular aging and osteoarthritis [22]. Additionally, DGCR8 contributes to DNA repair processes. Specifically, S153 phosphorylated DGCR8 participates in transcription coupled nucleotide excision repair in UV-induced DNA lesions, while S677 phosphorylation on DGCR8 upon radiation facilitates double-strand break (DSB) repair and enhances radioresistance [27,28]. Ever increasing number of studies reports on DGCR8's and the Microprocessor's emerging role in direct post-transcriptional regulation, particularly, mRNA splicing in the supraspliceosome. The supraspliceosome is a large RNP complex responsible for the pre-mRNA processing steps. It consists of uridine-rich snRNPs (U snRNPs), various splicing and alternative splicing factors, and other proteins that process the pre-mRNA [29]. Investigations revealed that DROSHA and DGCR8 are associated with the supraspliceosome, where pre-mRNA splicing and the processing of intronic miRNAs are coupled with an active cross-talk: changes in miRNA processing have significant effects on alternative splicing and vice versa [30–32]. A prominent example of *Dgcr8*'s additional role in gene regulation by alternative splicing is the T-cell factor 3 gene (*Tcf711*), which exists as two isoforms, each regulating mESC self-renewal but with opposing impacts on the regulation of their differentiation [33]. The Ciaudo group's 2017 study demonstrated that the *Dgcr8*-dependent splicing of the short isoform governing differentiation program is pivotal for the exit of pluripotent state [34], elucidating the differences between *Dicer* and *Dgcr8* knockout mESCs noted by the Blelloch group [9]. *Dgcr8* is also essential for the maintenance and differentiation during early corticogenesis through regulation of T-Box Brain Transcription Factor 1 (*Tbr1*) [35]. Surprisingly, *Dgcr8*'s involvement extends to LINE-1 (L1) regulation as well. The L1 mRNA is processed by the Microprocessor, subsequently regulating L1 and Alu retrotransposition *in vivo*. [36]. Notably, hyperactive retrotransposition was observed with L1 elements favoring regions harboring synapse- and schizophrenia-related genes.

Such hyperactive retrotransposition was also noted upon immune activation by poly-I:C [37]. Activation of Type I interferons has been known to inhibit Microprocessor [38], collectively suggesting DGCR8 haploinsufficiency's potential contribution to increased L1 retrotransposition. Interestingly, indications of L1 retrotransposition have emerged in various neurological disorders; many of them prevalent among DGS patients, including autism spectrum disorder (ASD), Alzheimer's disease (AD), major depression disorder and schizophrenia [37,39–45]. It is worth noting that the regulation of Microprocessor components operates through an auto-regulatory loop; DGCR8 is stabilizing DROSHA protein, and the Microprocessor is regulating *DGCR8* mRNA. The DGCR8 gene harbors two conserved hairpin structures, one in the 5'UTR and another in the second exon. Cleavage of these hairpins by the Microprocessor results in mature miR-1306-3p and miR-1306-5p from the downstream hairpin, while the 5'upstream product remains in the nucleus [46,47]. Recent findings from the Gregory group provided additional insights into Microprocessor regulation and the hairpins present in *DGCR8* mRNA. Their work revealed that the DGCR8:DROSHA stoichiometry determines the biochemical activity of the Microprocessor, excess DGCR8 resulting in irreversible aggregation of both Microprocessor components. This regulation can be governed by the 5' hairpin, which has been identified as a critical mediator of germ layer specification through a short but functional DGCR8 isoform that escapes autoregulation without the regulatory loops [48]. Mammalian DROSHA genes were also found to contain a hairpin spanning exon 7, influencing alternative or constitutive splicing. In human cells, Microprocessor promotes skipping of exon 7, while in mice this hairpin remains unprocessed [49]. However, the biological significance of this additional control of DROSHA expression is not been fully elucidated [50]. This intricate web of regulatory mechanisms adds depth to our understanding of the Microprocessor's role in gene expression regulation.

1.2. miRNAs

MicroRNAs (miRNAs) are a class of small non-coding RNAs that play pivotal regulatory roles in gene expression by targeting messenger RNAs (mRNAs) for degradation or translational repression [51]. In mammalian cells, mRNA degradation is the predominant mode of action [52,53]. miRNAs have emerged as essential regulators of diverse cellular processes, including cell differentiation, proliferation, apoptosis, and embryonic development [54]. miRNA-mediated gene regulation is intricate; a single miRNA can

target multiple mRNA molecules, and several miRNAs can also target the same mRNA [54–62]. Any dysregulation or alteration of miRNA expression can cause detrimental effects and may lead to the development of various diseases, including cancer and neurodevelopmental disorders [63–65]. It goes without saying that maintaining precise and regulated levels of miRNAs is crucial for normal cellular functions. Given the profound impact of miRNAs on gene regulation, they represent promising targets for disease diagnosis, prognosis, and therapeutic inventions.

1.2.1 miRNA biogenesis

The biogenesis of miRNA involves the following steps: transcription, nuclear processing, nucleocytoplasmic export, cytoplasmic processing, and the formation of the RNA-induced silencing complex (RISC). Both canonical and non-canonical pathways exist for miRNA maturation, each relying on different proteins and processing steps [66,67]. In the canonical pathway, the process begins with the transcription of primary miRNAs (pri-miRNA). The transcription from miRNA genes is often governed by tissue-specific superenhancers [68]. Subsequently, hairpin structures of the pri-miRNA undergo cleavage by the Microprocessor in the nucleus, resulting in precursor miRNAs (pre-miRNA) [69]. The Microprocessor complex comprises the RNase III enzyme called Drosha and its cofactor, DGCR8 [70]. Drosha cleaves the hairpin structures, giving rise to precursor miRNA (pre-miRNA). These resulting pre-miRNAs are then transported to the cytoplasm by Exportin-5 (XPO5) and RAN-GTP [69], where they encounter another RNase III enzyme, Dicer, for future processing [71]. This results in the formation of a short double-stranded RNA with two-nucleotide overhangs at its 3' end. This intermediate RNA subsequently associates with an Ago protein (AGO1-AGO4 in mammals) and its auxiliary factors, leading to the assembly of the functional RISC (see Fig. 1) [72]. In addition to the canonical pathway, non-canonical pathways for miRNA biogenesis have also been identified. Non-canonical miRNAs are derived from diverse sources, such as introns (Mirtrons), small nucleolar RNAs (snoRNAs), endogenous short hairpin RNAs (shRNAs) and transfer RNAs (tRNAs), among others [73]. Mirtrons are processed by the splicing machinery instead of the Microprocessor complex, yielding pre-miRNA-like hairpin structures with shorter stem [74–77]. These hairpins are subsequently exported to the cytoplasm and processed by DICER similarly to canonical pre-miRNAs (see Fig. 1). The snoRNA-derived miRNA pathway involves the processing

of snoRNAs into miRNAs [78]. Although snoRNAs are typically involved in RNA modification, they can also form hairpin structures and evolve into mature miRNAs through canonical processing [79–83]. Notably, DICER and DGCR8, components of the Microprocessor, not only process snoRNA-derived miRNAs, but can also stabilize mature snoRNAs [24,84,85]. Moreover, DGCR8 in conjunction with other proteins, governs the decay of mature snoRNA, thereby impacting the processing of miRNA derived from snoRNA [25]. tRNA-derived miRNAs arise from tRNA fragments, undergoing cleavage by DICER, before folded into a pre-miRNA-like structure that is further processed into mature miRNA [73]. A common attribute of the non-canonical pathways is their reliance on DICER. One exception is the processing of miR-451, which is cleaved by RISC components, namely Argonaute2 (AGO2) and the eukaryotic translation initiation factor 1A (EIF1A) [86,87]. While the roles of non-canonical miRNAs are still being investigated, they are believed to hold pivotal functions in gene expression regulation. These non-canonical miRNAs might exhibit distinct target specificity compared to canonical miRNAs.

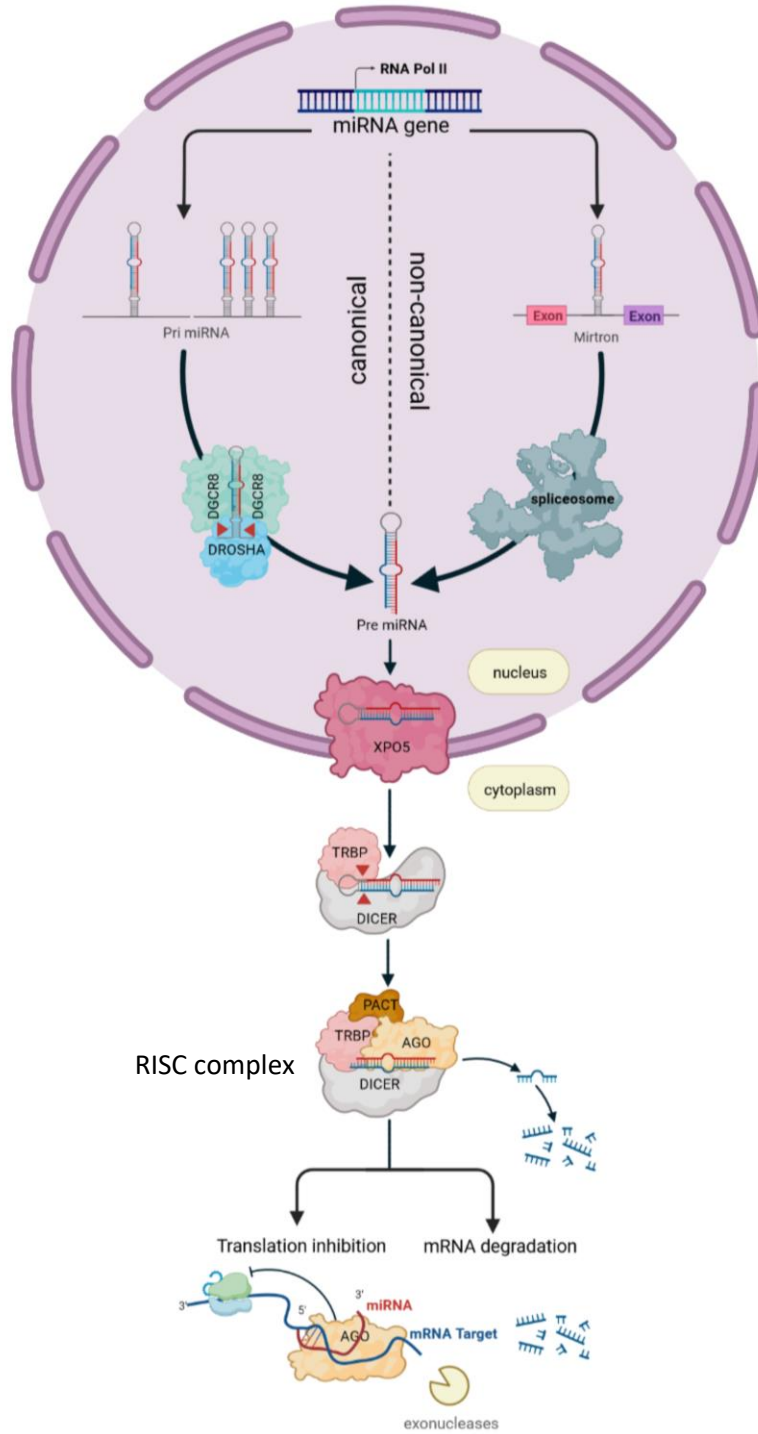


Figure 1. miRNA processing: Processing of the canonical miRNAs and mirtrons, a class of non-canonical miRNAs. *The figure was generated with Biorender.*

1.2.2 miRNA clusters

Recent analysis indicates that approximately half of the conserved human miRNAs organized in clusters within the genome [51]. In these clusters miRNAs are arranged in tandem and transcribe together as a polycistronic transcript [88]. While these clusters are typically small, comprising 2 to 8 miRNAs, there are also some remarkably extensive ones, such as chromosome 19 microRNA cluster (C19MC), which is specific to stem cells and placental tissue and contains 46 miRNAs [89,90]. Notably, members of a cluster tend to regulate functionally related biological processes and often consist of members from the same miRNA family, frequently also sharing a common seed sequence [51,91,92].

1.2.3 Posttranscriptional regulation of clustered miRNAs

The regulation of miRNA clusters is a complex and intricate process. Although miRNAs within a cluster are coordinately transcribed, mature miRNAs derived from the same transcript often exhibit distinct expression patterns, implying the existence of robust post-transcriptional regulation mechanisms [93–95]. The Microprocessor requires genetic and structural features in the pri-miRNA hairpins to recognize them thus for optimal processing. These features include a 35 ± 1 bp long stem, an unstructured apical loop ≥ 10 nt long and single stranded segments which are flanking the hairpin and ideal sequence motifs, like a basal UG motif, UGU/GUG on the apical loop [96]. Previously, miRNAs with poor structural features were thought to be processed through one of the non-canonical pathways. Subsequent research, however, showed, that these suboptimal miRNAs are enriched in polycistronic clusters. They are processed in conjunction with another member of the cluster, a proximal helper hairpin with optimal structure and motifs [97–101]. This phenomenon is referred to as ‘cluster assistance’. Recent studies have identified two proteins, the scaffold Attachment Factor B2 (SAFB2) and the enhancer of rudimentary homolog (ERH), as mediators of cluster assistance [98,101]. ERH binds to the N terminus of DGCR8 in 2:2 stoichiometry, while SAFB2 is a binding partner of ERH [98,102,103]. The precise mechanism and implications of ERH and SAFB2 in cluster assistance is yet to be defined. Shang et al. demonstrated, that this process involves the recruitment of the Microprocessor to the helper miRNA and subsequently to the suboptimal precursor [99]. Two theoretical models have been proposed: one involving Microprocessor dimerization and utilization of another Microprocessor for processing the

suboptimal, and the other involving a single Microprocessor complex that recognizes the suboptimal recipient before dissociating from the helper hairpin [101]. Beyond cluster assistance, various other factors may modulate the processing of individual cluster members. These include long noncoding RNAs, which can bind to individual miRNAs and increase or decrease their processing level [104,105]. Additionally, the circular RNA circLONP2 contributes to the upregulation of miR-17 by binding to the RNA helicase DEAD-Box Helicase 1 (DDX1) and ultimately DGCR8 [106]. Further RNA binding proteins, including heterogeneous nuclear ribonucleoprotein A1 (hnRNPA1) [107–110], also play roles in this regulatory landscape. As we have just seen, clustered miRNAs don't just act like independent units. Their regulation during miRNA processing forms a higher order scaffold involving numerous interacting partners, thereby enabling precise dosage control of miRNAs.

1.3. Human pluripotent stem cells

Stem cells are capable of differentiating into a diverse array of cell types in the body. Their classification is rooted on their plasticity, with decreasing developmental potency as one moves along the categories. Totipotent stem cells possess the extraordinary capacity to differentiate into any cell within the entire organism, including extra-embryonic structures. During development, blastomeres within the early stage morula are examples of totipotent cells. After approximately four days, as the blastocyst is formed, the inner cell mass transitions into pluripotent stem cells (PSCs) [111]. Pluripotent stem cells (PSCs) can give rise to all cell types of embryo, both somatic and germ cells [112]. Upon differentiating into one of the three germ layers, PSCs transform into multipotent stem cells, possessing the ability to generate cells belonging to specific lineages. An example is the hematopoietic stem cell, which is capable of producing various types of blood cells [113]. Lastly, unipotent stem cells exhibit the most confined differentiation potential, generating only one cell type [114]. While under well-defined conditions, PSCs can be cultured indefinitely *in vitro*, by modifying these conditions, they can be steered towards differentiating into representatives of all three germ layers. This exceptional attribute positions them as an inexhaustible source of cells for a myriad of applications, such as *in vitro* disease modeling, toxicological and pharmacological testing, and regenerative medicine [115].

1.3.1 Classification of pluripotent stem cells (hPSCs)

Pluripotent stem cells can be categorized into two types; embryonic stem cells (ESC), originating from the inner cell mass (ICM) of preimplantation embryos, and induced pluripotent stem cells (iPSC), which can be obtained by inducing the dedifferentiation of adult somatic cells by reprogramming (see Fig. 2) [116]. A significant turning point in the fields of cell and developmental biology occurred in 1998 when Thompson et al. isolated the first human ESCs (hESCs) fundamentally altering the landscape [112]. Since then, various comprehensive protocols have been developed for standard stem cell culture and the differentiation of human pluripotent stem cells [117]. Before 2007, hPSCs could only be derived from preimplantation embryos [118]; and to this day, hESCs are the ‘gold standard’ of human pluripotent cell lines. Nonetheless, ethical considerations tied to the destruction and use of human embryos have limited their extensive applications [119,120]. Another revolution in stem cell biology came with Takahashi and Yamanaka’s groundbreaking discovery, demonstrating that somatic cells can be reprogrammed into an embryonic stem cell-like state. This was accomplished by inducing the co-expression of four key transcription factors, Oct4, Sox2, Klf4, and c Myc [121]. These reprogrammed cells, termed induced pluripotent stem cells, share key similarities with ESCs in terms of pluripotency, self-renewal, and gene expression profiles. However, the cell type’s origin may influence the cellular and molecular characteristics of the resulted cell lines, and the reprogramming process is associated with the acquisition of genomic aberrations [122–124].

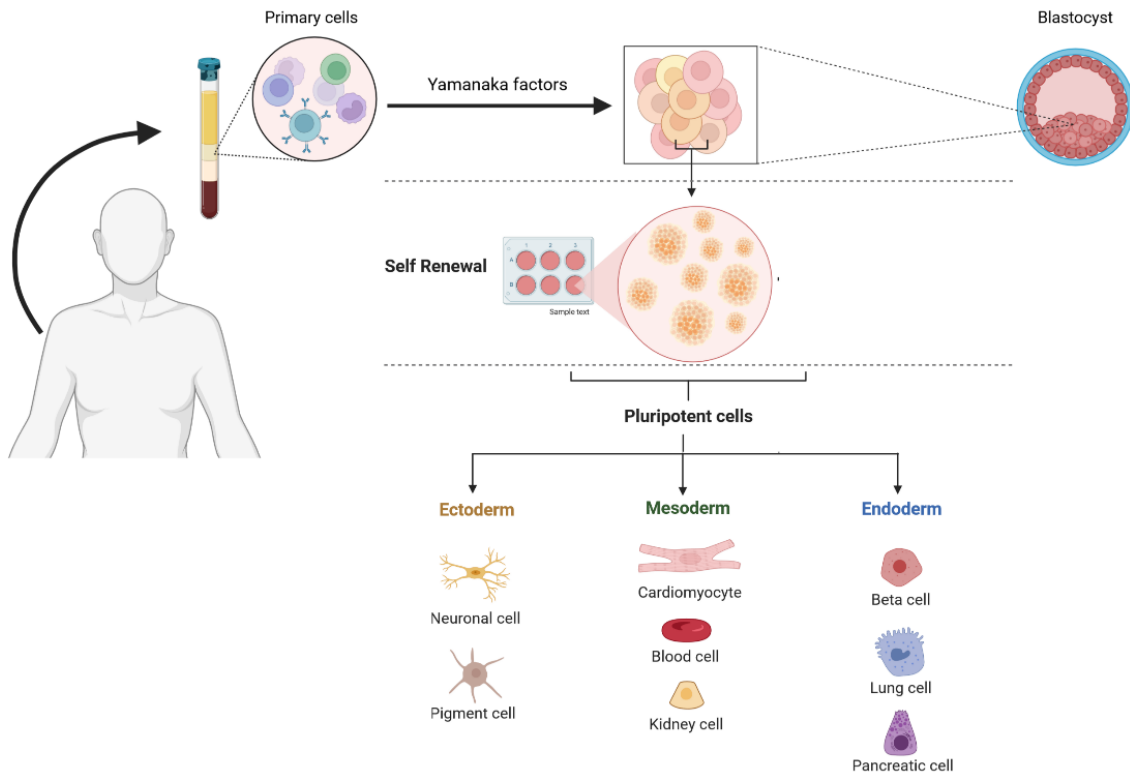


Figure 2. Pluripotent stem cells: Two types of human pluripotent stem cells: induced pluripotent stem cells (iPSC), which can be obtained by reprogramming primary cells, and ESCs, originating from blastocyst. Pluripotent cells have unlimited self-renewal and differentiative capacity towards the three embryonic germ layers. *The figure was generated with Biorender.*

1.3.2. Characterization of hPSCs

The maintenance of pluripotency relies on a distinct set of transcription factors and signaling pathways that govern the expression of genes responsible for self-renewal, differentiation, and maintenance of pluripotency [125]. Key genes and transcription factors associated with pluripotency include Oct-4, Nanog, Sox2, Rex1 [126]. Characterizing pluripotency in hPSCs can be performed using a variety of *in vitro* and *in vivo* methods. These include the alkaline phosphatase (AP) assay, embryoid body (EB) formation, *in vitro* differentiation, gene expression analysis, identification of surface antigens such as Tra-1-81, SSEA-4, and SSEA-3, as well as the presence of transcription factors mentioned earlier, and the formation of teratomas [125]. The AP assay is used to detect high activity of the enzyme in hPSCs, serving as an indicator of pluripotency [127]. Gene expression analysis confirms pluripotency by examining active gene patterns in

hPSCs. The expression of certain genes, including as Oct-4, Nanog, Sox2, and Rex1, can indicate pluripotency [128]. By assessing the levels of these genes and pathway activities, the pluripotent status of a hPSC line can be determined, and changes in gene expression during differentiation can be tracked [129]. Both teratomas and embryoid bodies (EBs) are utilized to characterize the spontaneous differentiation capacity of hPSCs. Teratomas are tumor-like structures that are composed of tissues derived from all three germ layers (endoderm, mesoderm, and ectoderm) in an unorganized manner. Pluripotent stem cells are harvested and injected into severe combined immunodeficient (SCID) mice, resulting in teratoma formation. The structures are then harvested and analyzed [130]. On the other hand, EBs resemble the early stages of embryonic development and are 3 dimensional structures formed through the spontaneous differentiation of PSCs *in vitro*. The analysis of these three-dimensional structures reveals the presence of cells from all three germ layers (endoderm, mesoderm and ectoderm) [131,132]. Furthermore, directed *in vitro* differentiation can induce hPSCs to differentiate into various cell types, such as neurons, cardiomyocytes and blood cells, by using specific media and growth factors [133–138]. The presence of these differentiated cells can further confirm the pluripotency of the stem cells.

1.3.3. Genetic engineering in hPSCs

Genetic modification of human pluripotent stem cells holds significant potential for advancing our understanding of disease mechanisms and facilitating novel therapeutic approaches (see Fig. 3).

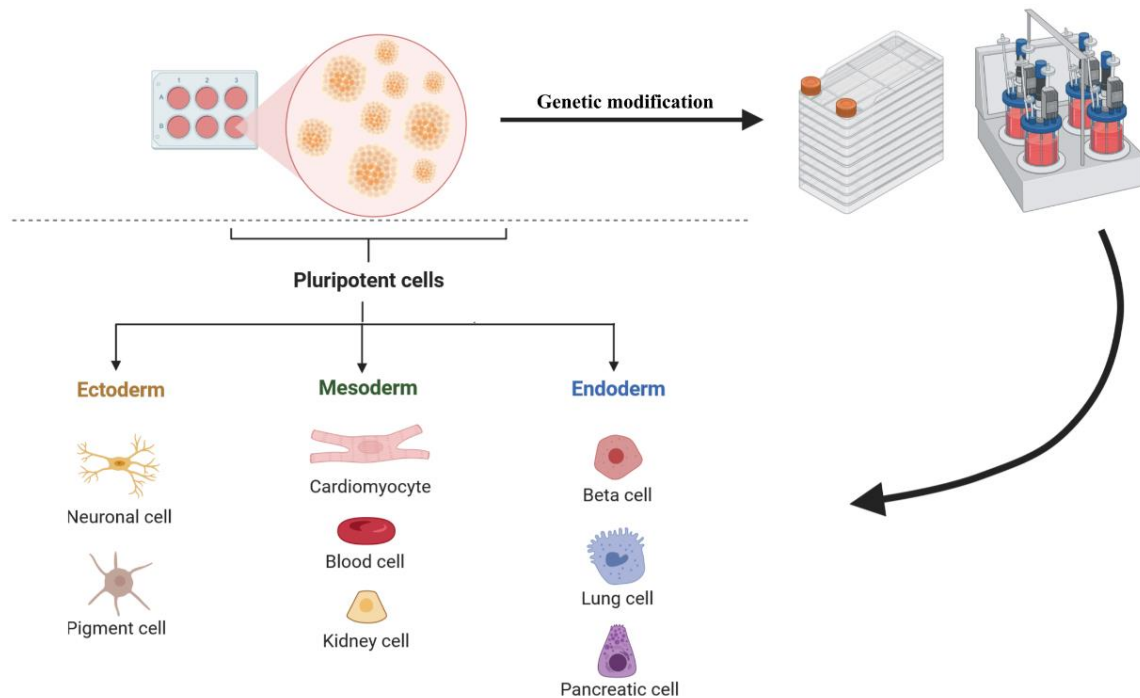


Figure 3. Significance of genetic modification in hPSCs: Genetically modified hPSCs serve as a promising tool for disease modeling and pharmacology: they can be cultured *in vitro* indefinitely providing large pools of mutant pluripotent cells, which later can be differentiated into any cell type originated from the three germ layers. *The figure was generated with Biorender.*

Methods involving viral vectors or transposons can enable stable gene expression through genomic integration, but lack the targeting of genomic editing [139–144]. On the other hand, genetic engineering techniques offer precise manipulation of the genome. Although genome editing strategies have evolved substantially in the last three decades, achieving targeted genetic modifications in hPSC and in selected genes can still prove challenging. Initial methods, such as homologous recombination (HR) without DNA cleavage posed limitations due to inefficient or random integration of donor sequences [145,146]. Recent

advances in site-directed nucleases, including zinc finger nuclease (ZNF), transcription activator-like effector nucleases (TALENs), and the CRISPR/Cas9 system have revolutionized the field by enabling base-pair precise double-strand break (DSB) induction and subsequent insertion of donor sequences through the cells' repair mechanisms. [147–150]. The CRISPR/Cas9 platform consists of two components, a single guide RNA (sgRNA) and a Cas9 endonuclease. The sgRNA, mimicking *trans*-activating CRISPR RNA (tracrRNA) – CRISPR RNA (crRNA) structure, contains a defined 20-nt spacer sequence, that complements the target sequence through standard Watson-Crick base pairing, followed by a downstream PAM (protospacer-associated motif) in the genome. A limitation of this technology is the need of a PAM as this motif is required for the target sequence to be recognized by the Cas9 protein as a potential target. For the widely used *Streptococcus pyogenes* (sp) Cas9, the PAM sequence is 5'-NGG-3' at the 3' end of the 20 nt target, but different Cas9 orthologs have varied PAM requirements [151,152]. In terms of workload, a typical CRISPR construct takes the preparation of the sgRNAs, whereas TALENs require protein engineering methods. On the other hand, off-target cleavage is more prevalent as for TALENs [153]. These off-target effects can result from mismatch tolerance between the spacer and target sequences or by the sgRNA sensitivity to the chromatin state [154]. To enhance targeting efficiency, strict selection of target sequences is required (38). For further improved specificity new strategies can be introduced, like delivery in ribonucleoprotein (RNP) complexes consisting of Cas9 protein and sgRNA, and the use of advanced Cas nucleases, like dimeric FokI-dCas9 or increased fidelity Cas9 nucleases [155–158]. Following double-stranded break (DSB) induction, major repair mechanisms come into play, including homology-directed repair (HDR) or nonhomologous end-joining (NHEJ) [159]. While HDR can integrate exogenous DNA donors seamlessly, NHEJ-mediated repair tends to form insertions or deletions (indels) at the repair site. These, if occurring in the coding sequence, often cause frameshift mutations and permanent gene inactivation [160]. The activity of the HDR and NHEJ pathways is highly context dependent. The predominant and robust NHEJ is the primary repair mechanism in the G1 phase, although it can be seen throughout the cell cycle [145,161,162]. On the other hand, HDR is mainly active in the S/G2 phase during cell division, making it far-fetched for postmitotic cells to employ [145,163]. In hPSCs, HDR-mediated insertions are especially rare when cells are not

synchronized in the G2/M phase [164], in fact, NHEJ-mediated insertion at target sites outperform HDR even with larger inserts [164–167]. In contrast, in mice, classical gene editing with HR has been successfully used for decades [168–170]. It is also worth mentioning that HR frequencies can vary considerably based on cell type, insert size, target accessibility, and chromatin state, respectively [171,172]. In general, the CRISPR/Cas9 platform offers a specific and precise genome editing with relatively high success rates and cost-effectiveness compared to other methods. Yet, frequencies of successful insertions in hPSCs remain lower than in other cell lines. Additionally, off-target and karyotype analysis are essential to detect unwanted genetic and chromosome alterations.

1.3.4. *In vitro* disease modeling with hPSCs

In the recent years, the use of embryonic stem cells (hESCs) and induced pluripotent stem cells (hiPSCs) for disease modeling has gained increasing attention [173]. These model systems involve the controlled differentiation of hPSCs into specific cell types that are often challenging to access directly from patients, allowing for an in-depth investigation of the underlying mechanisms and evaluation of potential therapeutic interventions. The distinct advantages offered by *in vitro* hPSC models over traditional animal models and primary cells are diverse. They reduced experimental costs and time-requirements, the capacity to generate substantial quantities of functional cells, and diminished ethical concerns related to animal welfare [174]. Notably, these *in vitro* human models hold the potential to yield more predictive responses, owing to the utilization of human cells. This potentially holds the promise of minimizing the gap between preclinical studies and clinical trials in the future [175–177]. An increasingly popular approach is the generation of patient-derived iPSCs, although this strategy does come with a set of associated challenges. Concerns related to genetic instability and the epigenetic status of the reprogrammed iPSCs, as addressed in section 1.3.1, underscored the need for stringent quality controls. Moreover, heterogeneity between the patient and healthy control cells due to genetic differences and cell line variations necessitates careful consideration [178–180]. High variability can pose challenges in data interpretation and can even make assays unfeasible.

For minimizing genetic variability and enabling genotype-phenotype associations, the establishment of isogenic cell line pairs has emerged as a pivotal strategy. These pairs, established through the induction of disease-associated mutations into healthy control lines or the correction of disease-linked mutations in patient-derived lines, offer a means of mitigating genetic variability and enabling robust genotype-phenotype correlations [149,181]. Such genetically engineered cells with induced monogenic mutations and knockout systems facilitate the investigation of the impact of individual mutations or genes on complex phenotypes. This approach is invaluable for understanding the underlying molecular mechanisms and identifying potential therapeutic targets. Additionally, these engineered cells serve as platforms for drug discovery, helping the identification of compounds that could be effective in rescuing the defected phenotype [182,183]. Numerous hPSC-based models have already been developed for a diverse spectrum of diseases. This approach is invaluable in untangling the underlying molecular mechanisms and identifying potential therapeutic targets [184–190].

Even though hPSC models are promising tools, these systems have clear limitations. One of the main critics is the tendency of hPSC-derived differentiated cells to display immature functional attributes [191–193]. The differentiation of hPSCs into fully mature progeny is a challenging task. In hiPSC-derived cardiomyocyte (hiPSC-CM) cultures, stimulation, electromechanical conditioning, small molecules, coculture with endothelial or fibroblast cells, and 3D culture together help to achieve the mature phenotype [194]. Similarly, modeling late-onset diseases is equally demanding, as evidenced by the efforts undertaken [188,195,196]. Notably, apart from maturity, the distribution of cellular subtypes within differentiated cultures often does not meet the physiologically relevant proportions. Addressing these concerns is vital for effective clinical translation [197–199,199–203].

In the broader context, *in vitro* disease models serve as potent tools for understanding the underlying disease mechanisms of specific disease-causing mutations, identifying potential therapeutic targets, and facilitating drug discovery. Their efficacy is especially pronounced when employed in conjunction with animal models and clinical observations, or when other model systems are unavailable. Future advancements will likely enhance our comprehension of genetic and cellular mechanisms and underlying cellular processes, thereby exceeding the limitations of this system.

2. Objectives

The ability to generate human embryonic stem cell (hESC) lines with specific genetic mutations has been a significant advancement in biomedical research. These cell lines serve as invaluable models for investigating early developmental processes, enabling studies that are difficult to perform *in vivo*. This dissertation is dedicated to bridge an important gap in knowledge by establishing and characterizing a hESC line with DGCR8 deficiency. Within the scope of this research, we pursued two primary objectives. Firstly, since human ESCs are prone to have enhanced repair mechanisms and are difficult to edit, we sought to determine the feasibility of employing a knock-in/knock-out approach using two tandem CAG-driven selection markers in the HUES9 human embryonic stem cell line, focusing on the DGCR8 gene. We also intended to characterize and register the resultant cell line in accordance with the rigorous criteria set for newly established stem cell lines. Secondly, given the profound biological significance of tightly regulated miRNA biogenesis during early embryogenesis, this work also addresses the question of how DGCR8 deficiency impacts the viability, maintenance of pluripotency and differentiation potential of the hESCs, the mRNA and protein levels of the Microprocessor components and the alterations of the functions of the miRNA machinery. In its entirety, this research contributes to the expanding knowledge regarding miRNA regulation and the role of DGCR8 in pathological phenotypes, such as those manifested in DiGeorge syndrome. Furthermore, the cellular model developed herein presents a novel platform for studying miRNA biogenesis in human pluripotent stem cells and their differentiation.

3. Methods

Cell Culture

The HuES9 hESC line was kindly provided by Douglas Melton and used according to the permission of ETT (approval number 6681/2012-EHR. HuES9). All the cell lines were grown on plates coated with Matrigel (Corning) and kept in mTeSR1 media (Stem Cell Technologies) with or without 0.8 μ M of puromycin (Thermofisher Scientific). Accutase (Thermofisher Scientific) was used to passage the cells and they were then plated in mTeSR1-Y media (mTeSR1 with 10 μ M Y27632-2HCl (Selleckchem). The genetic identity and normal karyotype were verified by STR analysis of 17 sites and G-banding, which was carried out by UD-GenoMed Medical Genomic Technologies Ltd.).

CRISPR/Cas9 genome editing

The sgRNA utilized for precise genome editing were designed using the guide design tool developed by the Zhang lab (accessible at <http://crispr.mit.edu/>). Based on the *in silico* predictions, we synthesized the five most promising and specific sequences to target the third exon of DGCR8. The designed oligonucleotides were cloned into the plasmid pX330-U6-Chimeric_BB-CBh-hSpCas9 (Addgene #42230). As for donor vector backbone, we employed a "self-cleaving" plasmid containing universal gRNAs. These facilitate efficient in-cell plasmid cleavage and thus eliminate the need for a linearized donor plasmid to achieve proficient targeted integration. [204]. An expression cassette containing two tandem, CAG promoter-driven selection marker genes -puromycin resistance and GFP- was cloned into this donor vector. Approximately 4×10^6 HuES9 cells underwent electroporation with the aforementioned two vectors. This was executed with an Amaxa Nucleofector using the Human Stem Cell Nucleofector Kit (Lonza), utilizing the A-23 program. After electroporation, the cells were seeded onto Matrigel-coated plates using mTeSR1-Y medium. The consecutive steps included puromycin selection and single-cell cloning based on GFP expression. Unintended cleavage and mutations at untargeted genomic sites were ruled out via sequence analysis of the top five *in silico* predicted off-target sites.

Single-Cell Cloning

Cells were separated using StemPro Accutase and single cells were plated in 96-well plates coated with Matrigel using a BD FACSAria™ cell sorter based on their expression of GFP in cloning media (mTeSR1-Y with 1/3 MEF-conditioned hESC medium). SSCs were grown in cloning medium for 10-20 days and then moved to 24-well plates coated with Matrigel in mTeSR1-Y medium. When the cells reached 80% density, they were transferred to 6-well plates. GFP expression was confirmed by FACS measurements.

Trichostatin A Treatment

Cells were placed in 6-well plates and grown without adding puromycin. On the third day, cells were treated with mTeSR1 medium containing either 30 nM or 60 nM Trichostatin A. The next day, the cells were removed and the GFP expression was measured in both treated and untreated control cells using flow cytometry. At the same time, the expression of the GAGE cancer testis gene was checked using RT-qPCR to confirm that TSA had effectively caused demethylation.

***In vitro* spontaneous differentiation**

The hESC colonies were separated using collagenase (ThermoFisher Scientific) and grown in suspension on plates that prevent attachment in EB medium (KO-DMEM with 20% FBS, 1 mM L-GLU, 1% non-essential amino acids and 0.1 mM β -mercaptoethanol) (ThermoFisher Scientific) for 6 days. Subsequently, the embryoid bodies (EBs) were moved to 24-well tissue culture plates or confocal chamber slides (Nalgene) coated with 0.1% gelatin (ThermoFisher Scientific) and allowed to differentiate for another 12 days in DMEM with 10% FBS. The derivatives of the EBs were examined by immunocytochemical staining and qPCR.

Immunofluorescent staining and flow cytometry

Cells were fixed, blocked, and permeabilized as described in [205]. They were then incubated with primary antibodies for 60 minutes at room temperature. After washing, the cells were incubated with corresponding secondary antibodies for 60 minutes at room temperature. Cell nuclei were stained with DAPI. For more details, see [205,206]. The SSEA4 flow cytometry analysis was carried out as described in [205].

RNA Isolation

Total RNA from hES and differentiated cells was extracted using TRIzol reagent (ThermoFisher Scientific). RNA integrity was checked using agarose gel electrophoresis and total RNA concentrations and sample purity were measured using a Nanodrop spectrophotometer (ThermoFisher Scientific).

miRNA analysis

For pri-miRNA analysis, 1 μ g of total RNA was reverse transcribed using random oligomers and a high-capacity cDNA Reverse Transcription Kit (ThermoFisher Scientific). cDNA samples were diluted 1:10 before amplification. For C19MC pri-miRNA, RT-PCR was performed using a SYBR Green PCR Master Mix with custom-made PCR primers. For mature miRNA quantification, the expression analysis was done using the miRCURY LNATM Universal RT miRNA PCR Assay (Qiagen) according to the manufacturer's instructions. RNA samples (5 ng/ μ L) were reverse-transcribed and the UniSp6 RNA spike-in template was added to each reaction to control the quality of cDNA synthesis. The cDNA samples were diluted 1:80 before amplification. RT-PCR was performed using a miRCURY SYBR[®] Green master mix (Qiagen) and real-time PCRs were performed on a StepOnePlusTM platform (ThermoFisher Scientific) according to the manufacturer's protocol. The hsa-miR-103a internal control miRNA was used for normalization during relative quantification using the $\Delta\Delta$ Ct method. For more details see [206].

Gene expression analysis (RT-PCR)

For gene expression assays, cDNA samples were created from 400 ng of total RNA using the Promega reverse transcription system according to the manufacturer's instructions. mRNA levels for *DGCR8*, *DROSHA*, *NANOG*, *AFP*, *TBXT*, and *PAX6* were determined using TaqMan[®] gene expression assays (ThermoFisher Scientific). Real-time PCR measurements were run and analyzed on the StepOneTM Real-Time PCR System (Applied Biosystems) according to the manufacturer's instructions. Quantitative gene expression data were normalized to endogenous control mRNAs: *RPLP0* or *Polr2A* for details of the Taq-Man[®] analyses; for SYBR Green assay, see [205,206].

Protein Analysis by Western blotting

Samples were sonicated and then run on 8% acrylamide gels before being electroblotted onto PVDF membranes. The membranes were blocked with blocking solution (5% Milk/TBS-Tween) and incubated with a monoclonal antibody specific to human DGCR8 (1:1,000, Abcam) overnight at 4 °C. Anti-rabbit IgG (1:5,000, ThermoFisher Scientific) was used as a secondary antibody. Pierce ECL Western blotting substrate (ThermoFisher Scientific) was used for signal detection and the membranes were exposed to Agfa films. An anti- β actin antibody (1:10,000, Abcam) was used to normalize the DGCR8 expression. Expression levels were determined by measuring the density of scanned images using ImageJ and correcting for background and normalizing to β -actin and parental HuES9 levels. The region of interest (ROI) for a given protein was chosen to be the smallest rectangle shape that could enclose the largest band of that protein and was used in all lanes of a blot. The background for normalization was measured using the same ROI near the target band, avoiding any specific bands if present. For more details, see [205,206].

4. Results

4.1. Establishment of the DGCR8 deficient hESC line

To generate the DGCR8 deficient hESC line, a CRISPR/Cas9-based knock-in/knock-out approach was utilized. To target DGCR8, a specific sequence was designed by identifying unique sequences in Exon 3. Targeting this region leads to the absence of functional protein expression on a disrupted allele while preserving the integrity of the two 5' autoregulatory loops [207]. Subsequently, these sequences were cloned into a px330 vector encoding the spCas9 nuclease (Addgene #42230). Additionally, a “self-cleaving” donor vector was constructed with two tandem CAG promoter-driven selection marker genes: puromycin resistance and GFP (Fig. 4).

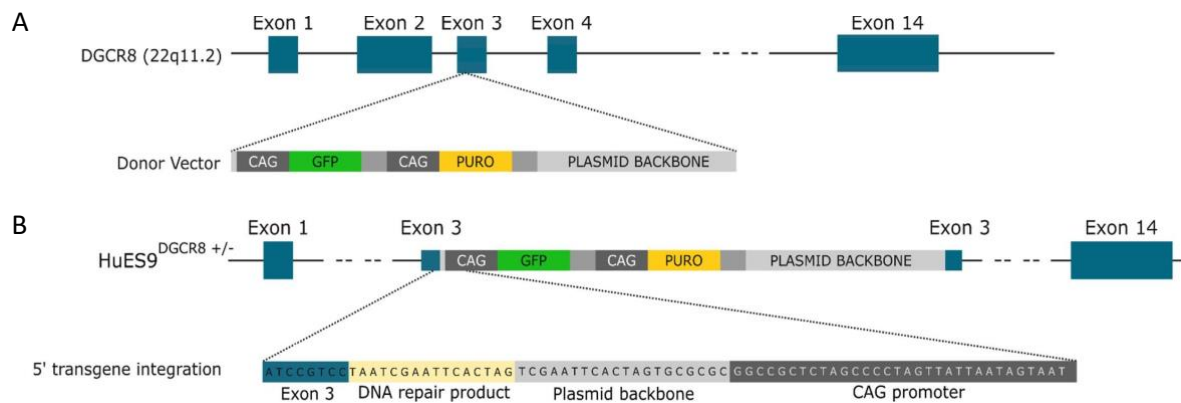


Figure 4. CRISPR approach and the transgene integration sites: Schematic overview of the (A) donor construction with the tandem, CMV-early enhancer/chicken β actin promoter (CMV) driven GFP and Puromycin resistance (PURO) genes and the (B) targeted region within the third exon of the DGCR8 gene [205].

HUES9 hESCs were subjected to electroporation using the two vectors, followed by puromycin enrichment of cells with stable marker expression. Subsequently, 100 single GFP expressing cells were isolated for clonal expansion. Out of the 100 clones, 20 could be successfully expanded and subjected to genotyping. We did not identify instances of biallelic insertions, yet one clone among the 20 showed monoallelic insertion. Sanger sequencing of the target site unveiled a 16 bp long NHEJ product upstream of the donor DNA as shown in (Fig. 4). Our analysis did not reveal indels or other insertions at the

predicted off-target sites (for detailed sequence alignment, please refer to [205]). These cells retained stem cell-like morphology as indicated in (Fig. 5 A), and maintained a normal karyotype as observed in (Fig. 5 B). These cells were also free of mycoplasma and STR analysis on 17 sites proved their identity (as detailed in [205]). The generated DGCR8^{+/-} cell line underwent comprehensive characterization in line with the strict requirements of pluripotency testing. This included the identification of key genes and transcription factors linked to pluripotency alongside carrying out a spontaneous differentiation assay. The resulting monoallelic hESCs showed robust expression of the pluripotency markers OCT4 and NANOG, with the additional strong expression of the surface antigen SSEA-4, further indicating their pluripotent state (Fig. 5 D, E, G). Upon induction of spontaneous differentiation, these cells displayed the expression of lineage-specific markers from all the three lineages: ectoderm (TUJ1, PAX6), mesoderm (TBXT, SMA), and endoderm (AFP) (Fig. 5 F, G). The decreased expression of DGCR8 protein was confirmed by Western blot (Figure 5 C). The cell line has been published [205] and registered under the unique identifier ‘HVRDe009-A-1’.

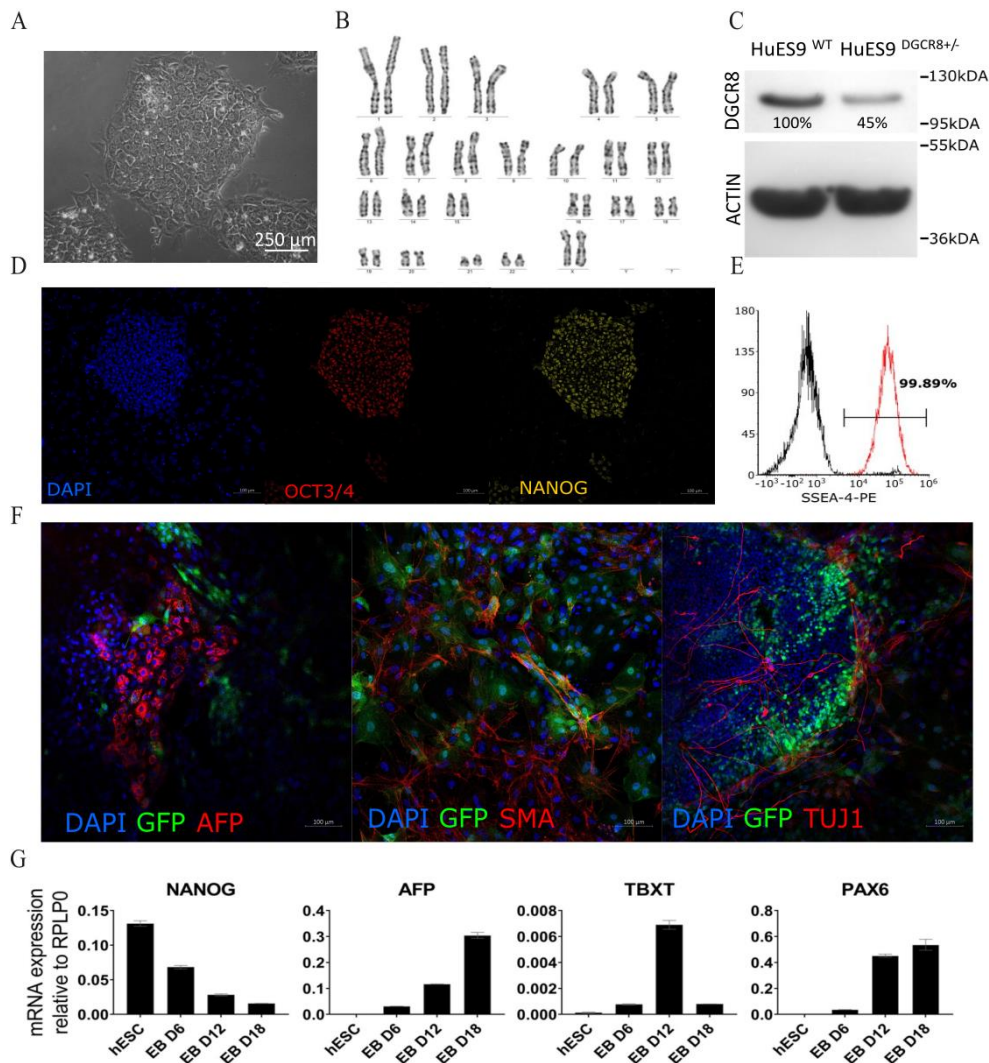


Figure 5. HVRDe009-A-1 colony morphology and karyogram: (A) HVRDe009-A-1 exhibits typical stem cell-like morphology and forms colonies. (B) Representative karyogram of the HVRDe009-A-1 cell line. Resolution 450-500 bands per haploid chromosome. (C) Representative Western blots for DGCR8 and β -actin. (D) Immunostaining of the pluripotency markers OCT4 and NANOG on the undifferentiated HVRDe009-A-1 cells (E) SSEA-4 flow cytometry analysis of undifferentiated HVRDe009-A-1 cells. (F) Immunostaining of markers specific for the three germ layers (AFP endoderm, SMA mesoderm, TUJ1 ectoderm) in differentiated offspring (embryoid body day 12). (G) relative mRNA expression to *RPLP0* housekeeping gene of pluripotency and lineage-specific markers on undifferentiated hESCs and differentiated offspring (embryoid body day 12), mean \pm SD values of technical replicates are shown [205].

4.2. Gradual loss of transgene expression in DGCR8^{+/-} hESCs

Consistent monoallelic expression of GFP was observed in HVRDe009-A-1 cells under puromycin-containing culture conditions (Fig. 6 A, B, C). However, after puromycin deprivation, GFP expression decreased gradually (Fig. 6 B). To investigate whether transgene silencing was a consequence of promoter hypermethylation, the cells were treated with Trichostatin A (TSA), a compound that promotes the removal of acetyl groups from histones. The treatment led to an increase in GFP expression only in cells that were still GFP-positive, thereby eliminating transgene silencing as the likely cause of GFP loss (Fig. 6 D). RT-qPCR measurements on FACS-sorted GFP negative populations showed a reduction in copy number, implying that genetic rearrangements and the loss of transgene copy from the DGCR8 locus were likely contributed to the loss of transgene expression (Fig. 6 E). Both GFP positive and GFP-negative single cells were selected and subsequently expanded for further characterization as illustrated in (Fig. 6 A).

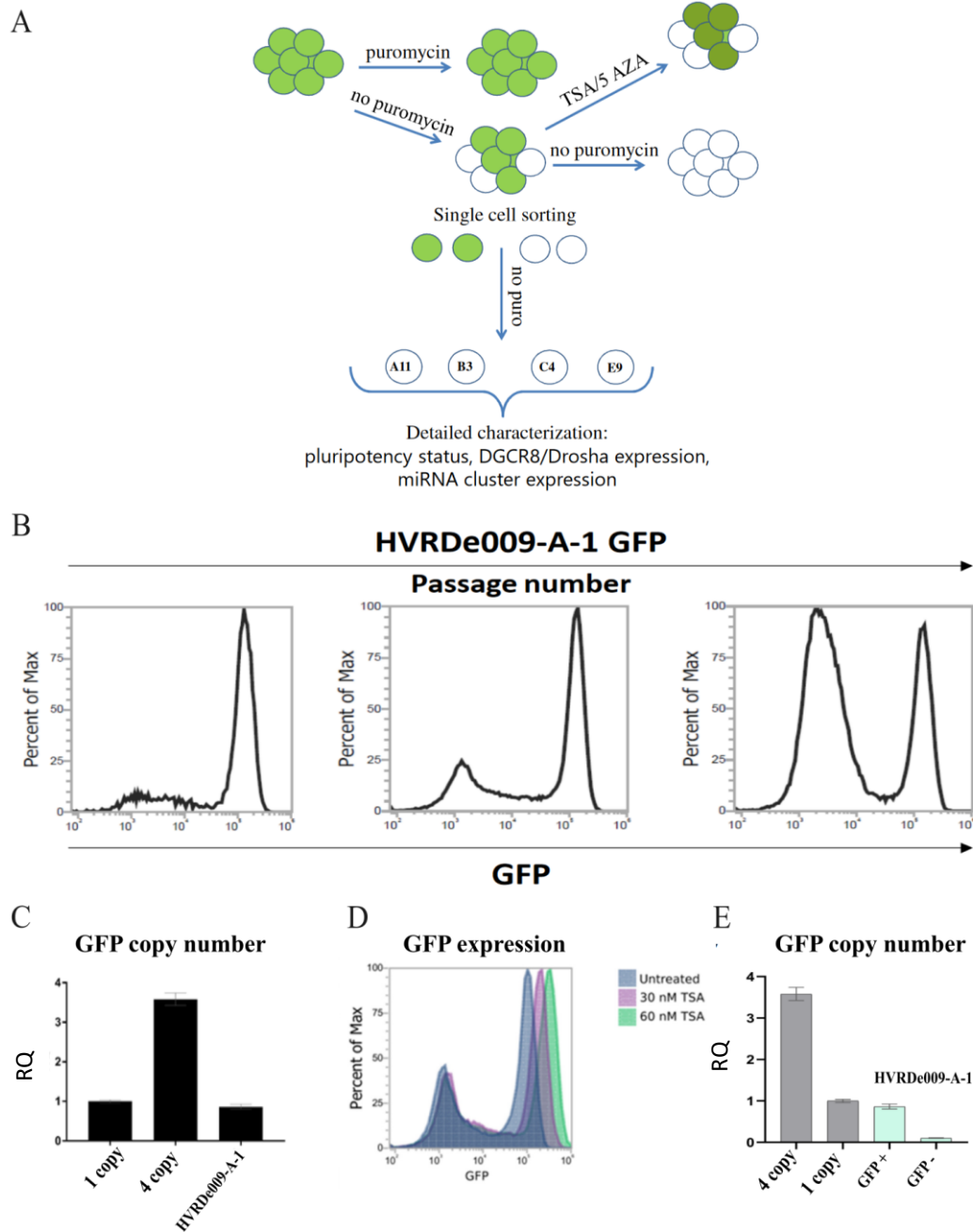


Figure 6. Gradual loss of transgene expression in the HVRDe009-A-1 cells: (A) Schematic overview of clone selection (B) GFP FACS measurements of cells during puromycin deprivation. (C) GFP copy number measurement in the HVRDe009-A-1 cells with antibiotic selection. Relative quantification (RQ) values were calculated using RPPH1 as reference target and a 1 copy control as reference sample; mean \pm SD values of technical replicates are shown. (D) GFP FACS measurements of cells treated with 0, 30 or 60 nM Trichostatin A (TSA), respectively. (F) Measurements of GFP copy number

in the GFP positive or negative sorted populations. Relative quantitation (RQ) values were calculated using RPPH1 as reference target and a 1 copy control as reference sample; mean \pm SD values of technical replicates are shown [206].

A total of 25 single cells were successfully expanded without puromycin selection. Among these, 12 of 25 had GFP positive origins and the remaining GFP negative. The progression of GFP loss during clonal expansion of GFP positive cells was closely monitored through FACS analysis. By day 30, GFP expression had dropped below 25% in 7 of 12 GFP-positive clones. Subsequently, by day 60, the expression had declined to 0% in two cases (as shown in Supplementary Fig. 1 and Fig. 7 A). In contrast, the GFP-negative clones retained the GFP-negative phenotype, irrespective of the presence of other parts of the insert. These findings were further confined by qPCR measurements, confirming the absence of the GFP expression cassette in the GFP negative clones (as illustrated in Fig. 7 B).

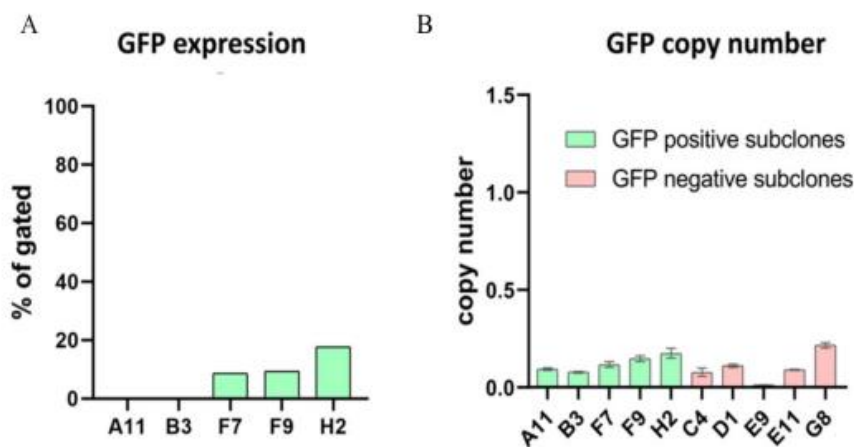


Figure 7. GFP expression and copy number in HVRDe009-A-1 clones: (A) GFP FACS analysis of GFP positive cell derived HVRDe009-A-1 clones 60 days after single-cell cloning. (B) Measurements of GFP copy number in the HVRDe009-A-1 clones 60 days after single-cell cloning. Relative quantification (RQ) values were calculated using RPPH1 as reference target and a 1 copy control as reference sample; mean \pm SD values of technical replicates are shown [206].

In general, the observations suggest that genetic rearrangements and the loss of transgene copy from the DGCR8 locus were likely the cause of the loss of transgene expression. The generated single cell clones were subjected to further genetic characterization.

4.3. Selected single cell clones contain certain regions of the insert.

Four single-cell clones (HVRDe009-A-1-A11, HVRDe009-A-1-B3, HVRDe009-A-1-C4 and HVRDe009-A-1-E9) were selected for further in-depth analysis. Every clone lost GFP expression and puromycin resistance along the clonal expansion without antibiotic selection (Fig. 8 A). To clarify the genetic mechanism for the loss of transgene expression, diagnostic PCR were conducted on these clones. Notably, substantial portions of both expression cassettes were found to be absent, resulting in the retention of specific segments of the integrated transgene (Supplementary Fig. 2). Through sequencing analysis, it was revealed that all four of the single-cell clones exhibited monoallelic disruption of the DGCR8 gene, while the intact allele remained preserved (Supplementary Fig. 3). Despite rigorous steps involving multistep FACS sorting and clonal expansion, these selected clones consistently maintained their characteristic stem cell-like morphology and normal karyotype (as shown in Fig. 8 B).

These results proved that the loss of transgene expression and puromycin resistance is due to genetic rearrangements and the loss of the transgene copy from the DGCR8 locus, rather than epigenetic silencing.

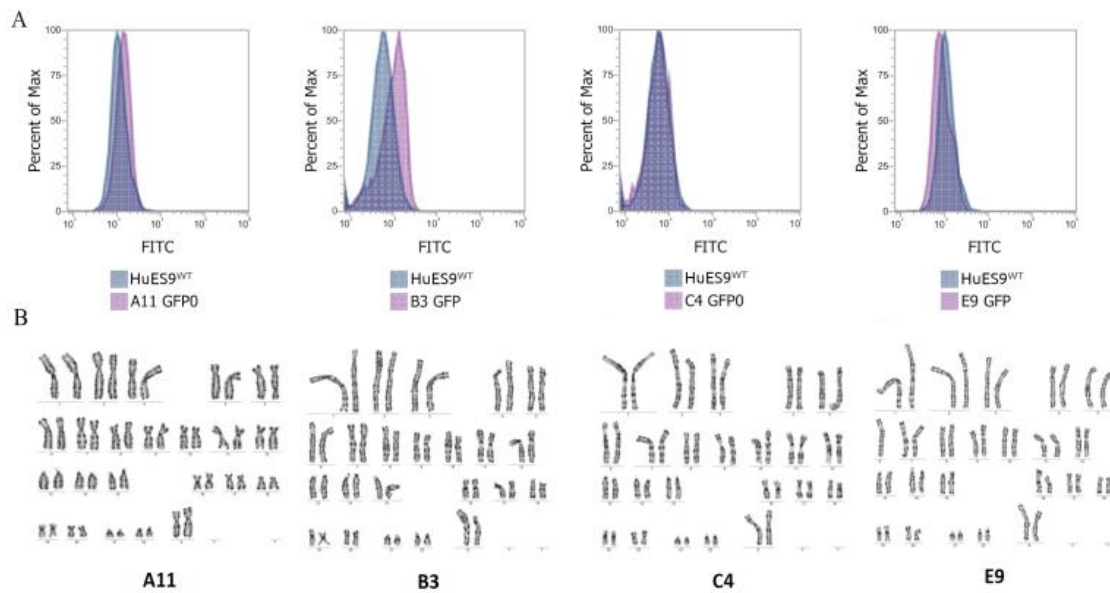


Figure 8. Expression of GFP and karyogram of the selected HVRDe009-A-1 clones: (A) GFP FACS analysis of the selected HVRDe009-A-1 clones (B) Representative karyogram of the HVRDe009-A-1 clones. Resolution 450-500 bands per haploid chromosome [206].

4.4. DGCR8^{+/-} hESCs maintain pluripotency and trilineage differentiation capacity.

The expression of crucial pluripotency markers, namely OCT4 and NANOG was thoroughly analyzed by immunostaining and real-time quantitative PCR. Remarkably, HuES9 DGCR8^{+/-} cells constantly expressed these markers, at levels comparable to the wild-type cell. This observation underscores that the introduced mutation did not affect the pluripotent state of the cells (Fig. 9 A and Fig. 10 B). Furthermore, flow cytometry analysis also demonstrated the robust expression of SSEA4 in cells, further confirming the cell's pluripotency (Fig. 9 B).

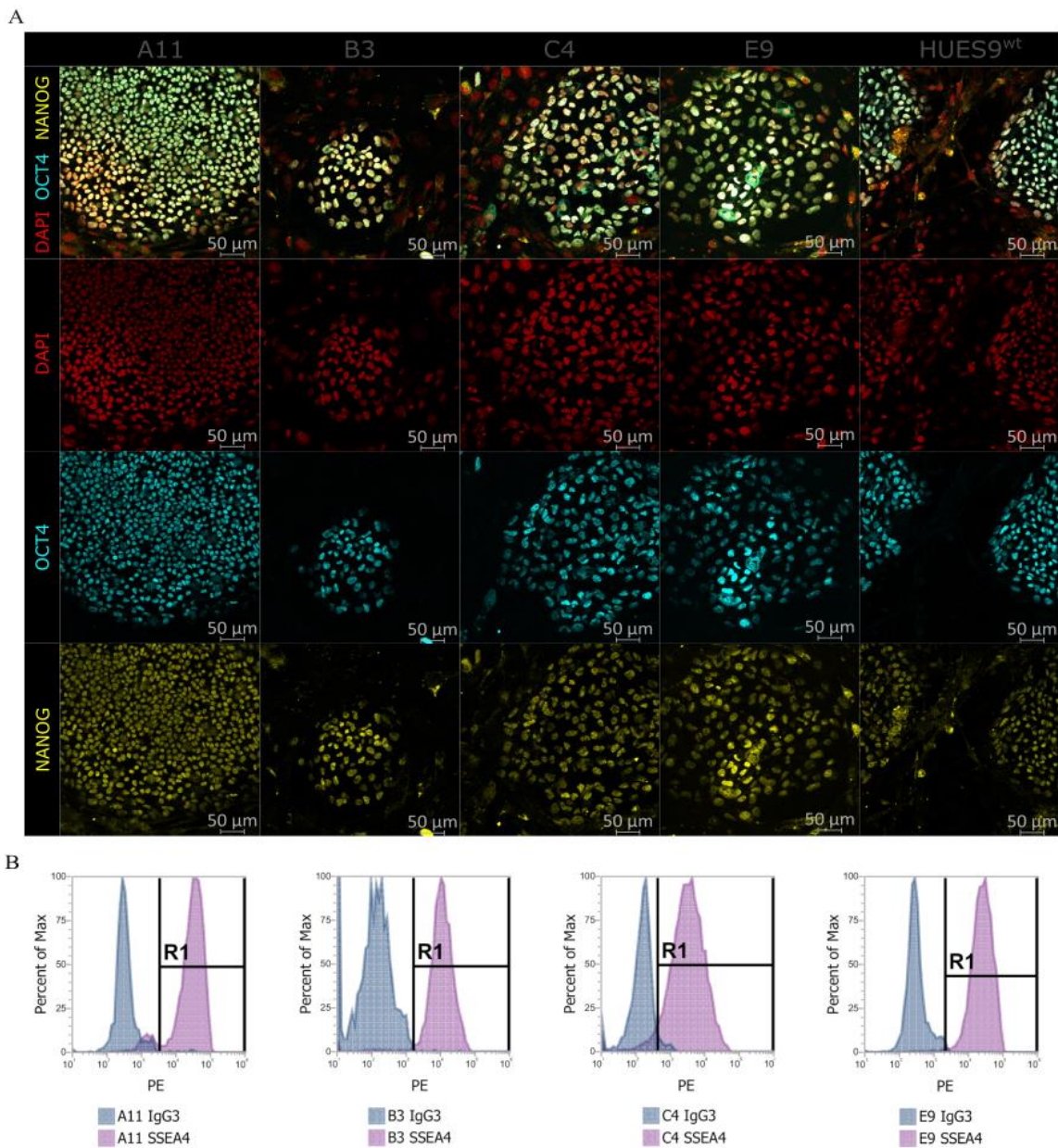


Figure 9. Pluripotency of selected HVRDe009-A-1 clones: (A) Immunostaining of the pluripotency markers OCT4 and NANOG on the undifferentiated HVRDe009-A-1 clones (B) SSEA-4 flow cytometry analysis of the selected HVRDe009-A-1 clones [206].

To investigate the differentiation potential of HuES9 DGCR8^{+/-} cells, embryoid body (EB) formation was used. Through this approach, markers indicative of the three germ layers -ectoderm (TUJ1, PAX6), mesoderm (TBXT, SMA), and endoderm (AFP) were detected by immunostaining and real-time quantitative PCR (Fig. 10). The clones displayed enhanced expression levels of OCT4 and NANOG in the undifferentiated state,

which progressively declined upon differentiation, as shown in (Fig. 9 A and Fig. 10 B). In contrast, differentiated offspring 12 days after EB plating presented increased expression in markers representing all three germ layers (Fig. 10).

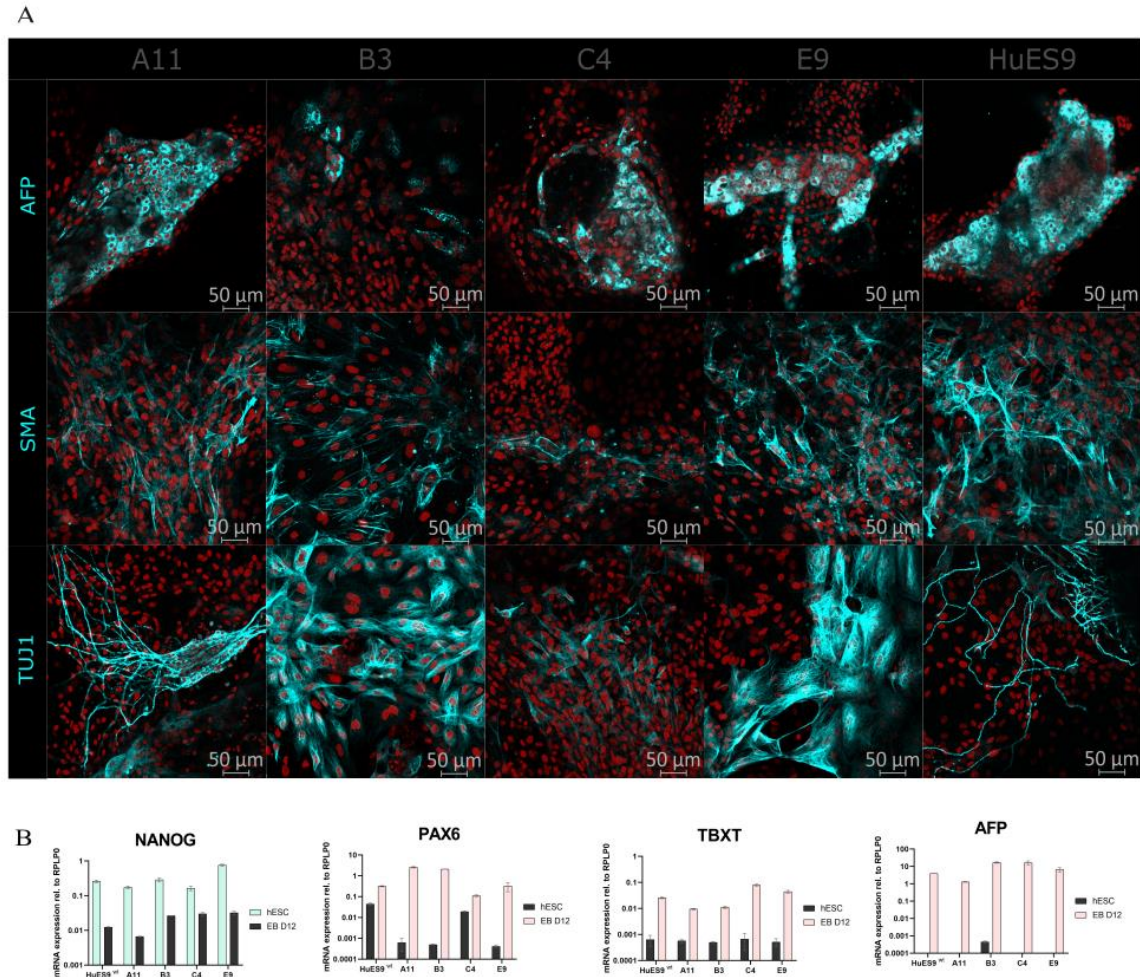


Figure 10. Differentiation capacity of selected HVRDe009-A-1 clones: (A) Immunostaining of markers specific for the three germ layers (AFP endoderm, SMA mesoderm, TUJ1 ectoderm) in differentiated offspring (embryoid body day 12); (B) relative mRNA expression to *RPLP0* housekeeping gene of pluripotency and lineage-specific markers on undifferentiated hESCs and differentiated offspring (embryoid body day 12); mean \pm SD values of technical replicates are shown [206].

Overall, these results demonstrated that the heterozygous deletion of *DGCR8* did not impair the pluripotency and spontaneous differentiation capacity of hESCs.

4.5. *DGCR8*^{+/-} hESCs show decreased *DGCR8* expression.

Given the complex autoregulatory loop between *DGCR8* and *DROSHA*, it becomes essential to evaluate the levels of *DGCR8* and *DROSHA* protein. Our methodology conducted concurrent measurements *DGCR8* and *DROSHA* within the same cellular population, thus providing a ‘snapshot’ of the clones. Notably the cell pellets utilized for both real-time quantitative PCR and Western blot analyses were derived from the same origin, ensuring accurate representation. Results of two representative experiments facilitated the following observations: Real-time quantitative PCR results showed slightly fluctuating levels of *DGCR8* in the clones, not considerably different in any case compared to the parental HUES9 line (Fig. 11 A and Supplementary Fig. 4 A). In contrast, Western blot detections consistently showed a reduction of 40-50% in protein expression within each clone relative to the parental line, regardless of the individual clone or its corresponding mRNA expression (Fig. 11 C and Supplementary Fig. 4 B). Meanwhile, the assessment of *DROSHA* mRNA and protein levels showed clone-specific expression profiles, clonal differences made comparisons with the parental HUES9 line inconclusive (Fig. 11 and Supplementary Fig. 4 A C).

These results show that in the expression profile of Microprocessor components on the mRNA level may be inconclusive. Compared to the parental HUES9 hESC line, every hemizygous clone showed indistinguishable *DGCR8* and *DROSHA* mRNA levels. The *DGCR8* protein levels, however, showed 40-60% reduction.

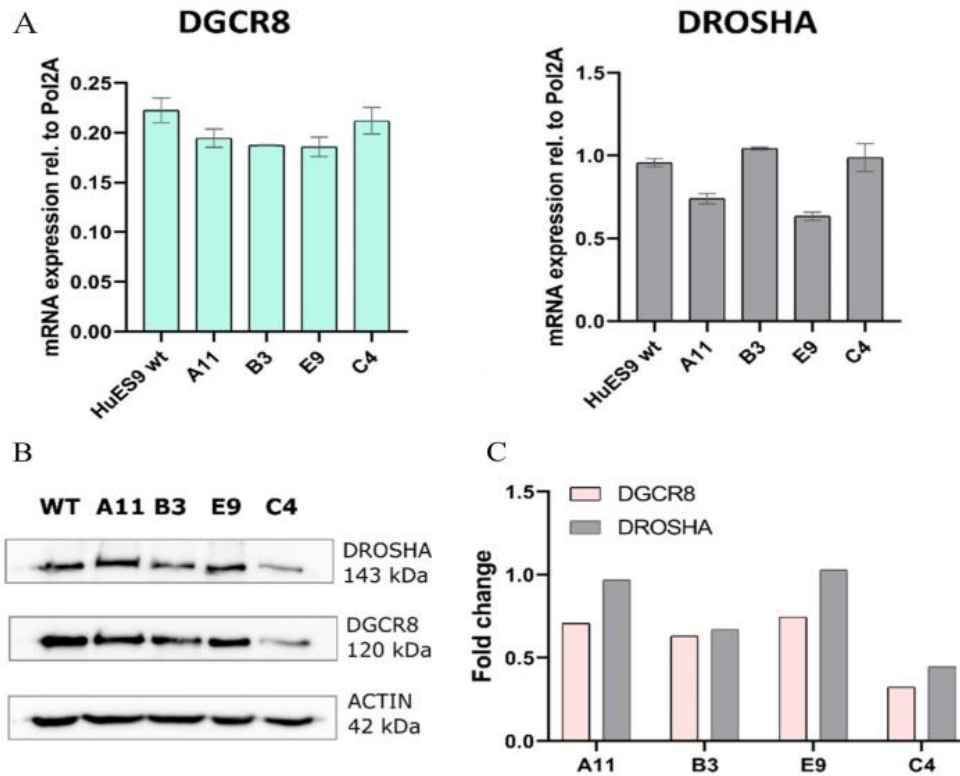


Figure 11. Expression of the Microprocessor components DGCR8 and Drosha in the selected HVRDe009-A-1 clones: (A) Expression levels of *DGCR8* and *DROSHA* mRNAs relative to *POL2A* endogenous control in a representative experiment; mean \pm SD values of technical replicates are shown. (B) Representative Western blots for DGCR8, DROSHA, and β -actin. (C) DGCR8 and Drosha protein levels of representative Western blots normalized to β -actin levels, and relative expressions in the parental HuES9 (WT) cell line [206].

4.6. DGCR8^{+/-} hESCs show partial disturbance of Microprocessor function.

The Microprocessor complex is essential for the processing of primary microRNA into mature miRNA. As clustered miRNAs share primary transcript, processing steps can provide an additional layer for their regulation. A previous study has shown that Drosha depletion by siRNA silencing in hESCs results in a gradual decrease in pri-miRNA processing in the extended miRNA cluster, C19MC [208]. Building upon these insights, we addressed the question whether partial depletion of DGCR8, the other essential component of the Microprocessor complex, may yield a similar phenotype. Therefore, we examined the processing activity in three selected regions along C19MC in four DGCR8^{+/-} clones. The results indicated clone-specific responses: clones E9 and B3

showed a modest, gradual decrease toward the 3' end of the cluster, while this decrease was not observed in clones A11 and C4, as shown in Figure 12. Interestingly, our findings did not demonstrate a clear correlation between DGCR8 expression levels and the observed responses. However, they do suggest a potential disturbance in the Microprocessor function among cells where the DGCR8 protein level is reduced due to a heterozygous mutation.

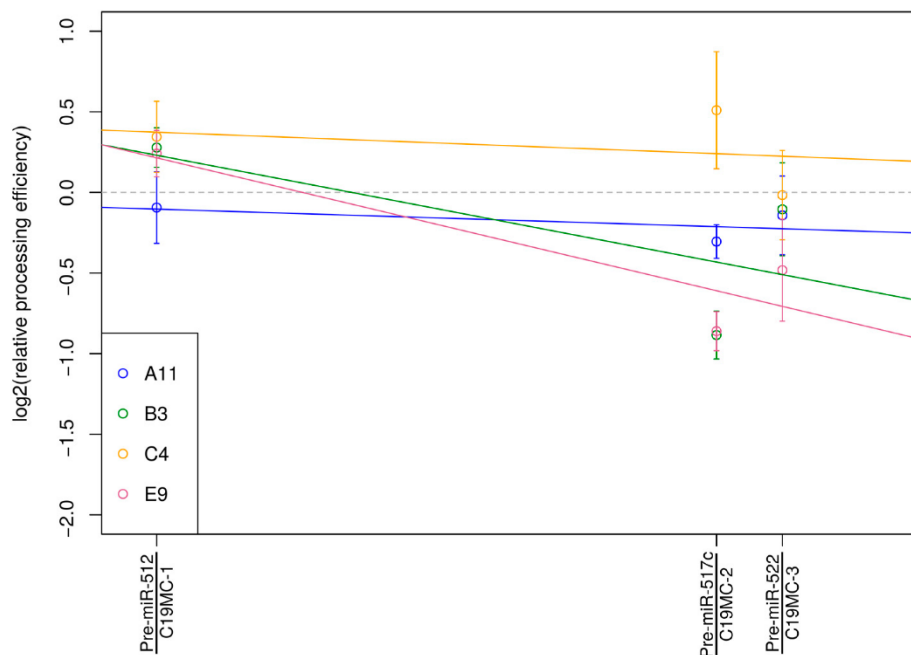


Figure 12. miRNA processing along the C19MC in selected HVRDe009-A-1 clones: Measuring position-dependent pri-mRNA processing along the C19MC in DGCR8 mutant clones. At 3 selected positions, the ratio of total versus unprocessed pri-miRNAs was determined using distinct primer pairs by real-time PCRs. In this representative experiment, colored circles show mean values of measurement points in different clones; \pm SD values of 3 technical parallels are also shown. Colored lines indicate the tendency to decrease in processing efficiency (if any) for a given clone. [206]

5. Discussion

miRNAs exert their function in the post-transcriptional regulation of gene expression. They have been proven to influence many important biological processes, including cell differentiation, proliferation, apoptosis, and embryonic development [54]. A dysregulated miRNA pattern is often implicated in various diseases, suggesting the crucial role of miRNA dosage in pathophysiological processes (202–205). The primary emphasis in research has traditionally been on mechanistic investigation of miRNA function. However, it is equally important to understand the importance of alterations in their coordinated regulation in disease pathogenesis. [67]. Pri-miRNA processing is one such regulatory step, carried out by the Microprocessor complex consisting of two components, DROSHA and DGCR8 [209]. DGCR8 is one of the genes affected by DiGeorge syndrome (DGS), a congenital disease caused by hemizygous microdeletions in 22q11.2 [2]. Major clinical manifestations in DGS include congenital heart disease, palatal abnormalities, immune deficiency, facial features, and central nervous system anomalies, among others [210]. Since 2007 various *Dgcr8* knockout model approaches have been established on mice and mESCs. Most of these studies concentrated on conditional- or tissue-specific knockout mice and mESCs [11–15]. While these models indeed provide an ideal platform for studying DGCR8 protein, non-canonical miRNAs, or non-canonical DGCR8 functions, they have less impact on the interpretation of the partial DGCR8 disruption presented in DGS. Studies concerning the consequences of monoallelic DGCR8 expression predominantly use mESC-derived neural cultures or mice for studying DGS or SCZ. They often find overlapping phenotype with DGS mouse models, including signs of altered brain miRNA biogenesis [17–21]. It is noteworthy that transcriptional networks and signaling pathways of mouse and human PSCs display considerable divergence due to species differences, making mESCs less reliable as models of human disease [211,212]. To our knowledge, only two papers have been published with partial or complete loss of DGCR8 in human pluripotent stem cells. The first reported altered cell cycle and poor self-renewal capacity coupled with spontaneous differentiation in *DGCR8*^{-/-} hiPSCs [22]. The other reported overlapping phenotypic alterations when comparing DGS- and *DGCR8*^{+/-} hiPSCs-derived cortical neurons further suggesting the prominent role of DGCR8 in DGS. However, the characterization of the haploinsufficient pluripotent stem cells was beyond the scope of these works [23].

This work presents the establishment and characterization of a DGCR8 hemizygous hESC line, a cellular tool to model DGS and linked psychiatric diseases, and to carry out comprehensive studies in miRNA biology. Human ESCs have enhanced repair mechanisms compared to their differentiated offspring and to hiPSCs, making them difficult to edit [213]. Therefore, we applied a knock-in/knock-out NHEJ approach with two tandem CAG-driven selection markers enabling GFP expression and puromycin resistance (Fig. 4 A). Despite our impressive transfection efficiencies, stable integration of our selection markers proved to be surprisingly low, even though NHEJ delivery of large inserts was reported to be efficient [165]. With the help of multi-selection enrichment, in a stable GFP-expressing population, insertional events could be detected, and single cell clones of GFP-expressing cells established. Clonal expansion resulted in 20% survival, and the clones exhibited uniform and stable GFP expression. This meets the typical recovery of wild-type hESCs using mouse embryonic fibroblast-conditioned medium (MEF-CM) and Matrigel coating [214]. We could not detect clones carrying biallelic insertion. Given that biallelic insertions are generally less frequent and DGCR8 knockout ESCs and DGCR8^{-/-} cells have low proliferation rate, this is not surprising. PCR genotyping and Sanger sequencing revealed that 1 of 20 clones contained the insert in the right location (Fig. 4). The resulting cell line, HVRDe009-A-1, maintained stem cell-like morphology and normal karyotype despite the transfection, multistep FACS sorting, puromycin selection and single cell cloning (Figure 5 A B). All of this poses a high risk of developing karyotypic aberrations [215,216]. What is more, none of the top predicted CRISPR off-target sites carried mutations (for detailed sequence alignment see [206]). This was expected, given that ESCs, in general, have superior DNA repair machinery, and hESCs, unlike hiPSCs, have been reported to repair DSBs predominantly via homologous recombination repair (HRR) and high-fidelity NHEJ [217,218]. The HVRDe009-A-1 cells display uniform GFP expression in puromycin containing selection medium (Figure 6 B). However, without puromycin, cells slowly lose transgene expression (Figure 6 D). This could be caused by transgene silencing, which is known to occur in transfected cells; however, it is very unlikely, given the fact that the CAG promoter is known to sustain expression in PSCs [219]. Further genetic characterization on single cell clones of HVRDe009-A-1 revealed that loss of transgene expression is caused by genetic rearrangements resulting in the loss of significant portions of both

marker expressing units from the DGCR8 locus (Supplementary Fig. 2). Loss of heterozygosity is known to occur in PSC systems; however, this form of partial transgene loss differs from those observed in LOH [220]. Sanger sequencing data provided evidence for the sustained monoallelic disruption of DGCR8 in the subclones (Supplementary Fig. 3 B) which may be the consequence of the recombination of two identical CAG promoters. With this method, we generated mutated clones without selection markers. To date there is no other work studying the pluripotency and the differentiability capabilities of DGCR8^{+/-} hESCs. The knockout mESCs revealed that complete depletion of Dgcr8 is coupled with altered cell cycle, and that these cells are incapable of silencing their self-renewal program [9]. Consistent with hemizygous mESCs, The HVRDe009-A-1 clones show homogeneous expression of OCT4 and NANOG pluripotency markers in the hESC colonies, and more than 90% of the cells express SSEA-4 comparable to HUES9^{wt} (Fig. 9 A B). Their spontaneous differentiation capacity was tested using embryoid body (EB) differentiation (Fig. 10). We analyzed the presence and cellular location of markers specific for all three germ layers with immunostaining and RT-qPCR in parallel. None of the subclones showed any difference in the expression of markers of ectoderm (TUJ1, PAX6), mesoderm (TBXT, SMA), and endoderm (AFP) compared to the HUES9 cells throughout the differentiation process, indicating that monoallelic DGCR8 disruption is not sufficient to abort spontaneous trilineage differentiability potential (Fig. 10). This is in line with studies on hemizygous mice and mESCs. While all of them display strong and relevant pathophysiological phenotypic differences in differentiated neurons compared to controls in terms of synaptic plasticity and morphology, their differentiation towards neuronal lineages is intact except for alterations in progenitor proliferation [17–21]. Due to the autoregulatory feedback loop (discussed in detail in 1.3.1), the expression levels of DROSHA and DGCR8 are not implicit in DGCR8 hemizygous cells. *Dgcr8* mRNA levels were not included in those studies conducted on haploinsufficient mice except for a few examples: the Zakharenko group reported significant, around 20% decrease in *Dgcr8* mRNA levels in a *Dgcr8*^{+/-} mutant mouse model they generated; source of the sample was not published [20], while the Kim group found no significant differences on hemizygous mESCs in *Dgcr8* mRNA levels compared to those in wild-type cells [47]. Our results on *DGCR8* mRNA expression are consistent with those observed in these mice/mESCs: all four *Dgcr8*^{+/-} clones show slightly fluctuating but not

considerably different DGCR8 mRNA levels when compared to the parental HUES9^{wt} cells (Fig. 11 A, Supplementary Fig. 4 A). However, DGCR8 protein levels of DGCR8 are approximately 50% reduced in all cell lines compared to parental DGCR8^{+/+} ($n_{\text{total}}=10$ in 4 representative runs) (Fig. 11 B, Supplementary Fig. 4 B). Surprisingly, *DROSHA* mRNA and protein levels were not consistent with *DGCR8* protein decrease despite the well documented autoregulatory loop (Fig. 11 A C and Supplementary Fig. 4 A C) [47]. It is widely accepted that mRNA levels in DGCR8^{+/-} cellular and mouse models represent constant DGCR8 dosage. A 2011 study from the Blelloch group illustrates well the significant impact a 20-day long period over postnatal development can have on the cortex of Dgcr8^{+/-} mice: “Surprisingly, on postnatal day (P)5 Dgcr8^{+/-} frontal cortices showed no significant changes in *Dgcr8* mRNA levels assessed with quantitative PCR (qPCR).” “In contrast, by P25, *Dgcr8* mRNA was significantly downregulated by $40 \pm 9\%$ in Dgcr8^{+/-} cortex.” [221]. This strongly indicates that cell type and developmental state may considerably change *DGCR8* mRNA expression. In neurons, DGCR8 haploinsufficiency was reported to cause significant alterations in miRNA biogenesis, Ca²⁺ handling, proliferation [17–21]. Pri-miRNA processing is known to act as a regulatory factor in miRNAs [222]. Since clustered miRNAs share primary transcript, processing steps in their regulation are particularly important [46]. One of such clusters is the primate-specific C19MC, a large cluster of 46 miRNAs. It is predominantly expressed in hESCs and in the reproductive system, including the placenta [89]. A previous study found that the processing of the cluster members shows a position-dependent profile with decreased activity towards the 3' regions in hESCs, but not in placenta-derived cells. Additionally, this phenomenon could be enhanced with siRNA knockdown of DROSHA [208]. Therefore, we addressed the question whether haploinsufficiency in DGCR8, the other essential component of the Microprocessor complex, may cause a similar phenotype. Surprisingly, our results did not demonstrate a clear correlation between DGCR8 protein levels and the observed response, while two clones showed a modest, gradual decrease toward the 3' end, this could not be observed in the other two clones (see Fig. 12). This suggests a potential disturbance in the Microprocessor function among DGCR8 heterozygous cells. In the C19MC, tissue-specific differences in the effective Microprocessor recruitment to transcriptional sites are thought to influence processing of the primary transcript [208]. The limited

availability of any Microprocessor component can indeed act as a bottleneck. A previous study on the Microprocessor dynamics showed that DGCR8 is massively recruited close to the C19MC transcription sites and is also essential for DROSHA recruitment [223]. In addition, they are dissociating separately from the transcription site, and DGCR8 has a longer residue time [223]. Recently it was also found that ERH and SAFB2 recruit the Microprocessor by binding to the N-terminus of DGCR8 and mediate the processing of suboptimal and neighboring hairpins in miRNA clusters. Both ERH and SAFB2 tend to dimerize, suggesting a complex with a dimerized Microprocessor [224]. Furthermore, cluster assistance has been proved to effectively enhance processing over 1kb spacing between helper and recipient hairpins [101]. It is tempting to speculate that DGCR8 - due to its intensive recruitment by ERH - tends to be enriched on the processing site, while DROSHA dissociates. In this scenario, with locally increased DGCR8 levels in proximity to a polycistronic locus, processing could be feasible even with globally reduced DGCR8 levels. However, our knowledge of cluster assistance and the regulation is incomplete and fragmented. Countless trans factors may alter the Microprocessor recruitment, affinity, or cleaving activity. Dicer processing and decay further complicate the regulatory network. However, it is important to study the regulatory processes of miRNA biogenesis in different contexts. In summary, this study demonstrates that the hESC line with a heterozygous mutation in the DGCR8 gene serves as an effective molecular and cellular model for examining the functions of DGCR8. The suppressed maturation of canonical miRNAs resulting from lower DGCR8 expression also facilitates the study of noncanonical miRNAs. In general, the HVRDe009-A-1 cell line contributes significantly to understanding of the canonical human RNA interference pathway and the “noncanonical” functions of the DGCR8 protein.

6. Conclusions

This dissertation aims to focus on the establishment and characterization of a DGCR8 hemizygous hESC line. Employing our knock-in/knock-out NHEJ approach with two tandem, CAG driven selection markers (GFP expression and puromycin resistance), we successfully generated a GFP expressing monoallelic DGCR8 mutant clone (HVRDe009-A-1). This underscores the feasibility of this method for site-directed mutagenesis in hard-to-edit genomic regions. We observed spontaneous loss of transgene expression caused by genetic rearrangements, and the loss of significant portions of both marker-expressing units in the clonal derives of HVRDe009-A-1. Sanger sequencing provided evidence for the sustained monoallelic disruption of DGCR8 in all investigated single cell clones, enabling their future use in fluorescent assays. miRNAs play a pivotal role in the post-transcriptional regulation of gene expression; disruption of miRNA regulation may lead to differentiations defects. Our results show that haploinsufficiency in DGCR8 is not sufficient to disrupt the pluripotent state or the trilineage differentiation potential of hESCs, which is in line with the studies on *Dgcr8*^{+/-} mESCs. Given the overall phenotype, we assessed the question whether monoallelic DGCR8 expression is complemented by regulatory mechanisms or results in a substantial reduction in mRNA and protein levels. Intriguingly, while HVRDe009-A-1 cells and their progeny did only show minor disparities in *DGCR8* mRNA expression, protein levels exhibited approximate 50% reduction compared to wild-type parental cells. This discrepancy between mRNA and protein levels highlights the potential inconclusiveness of mRNA measurements alone. Lastly, a previous study found that processing of the primate specific C19MC cluster members shows a position-dependent profile with decreased activity towards the 3' regions in DROSHA knockdown hESCs. We investigated whether DGCR8 haploinsufficiency, as the other essential component of the Microprocessor complex, could yield a similar phenotype. Surprisingly, our results did not demonstrate a clear correlation between DGCR8 protein levels and the observed response. While two clones showed a modest, gradual decrease toward the 3' end, this could not be observed in the other two clones. Consequently, further comprehensive studies are needed to decipher the exact processes behind the incomplete penetration of this phenotype.

In summary, the main findings of this study as follows:

- Insertional mutagenesis via CRISPR/Cas9 and NHEJ repair is a viable approach to induce monoallelic loss-of-function mutations.
- *DGCR8*^{+/-} hESCs effectively maintain their pluripotent state.
- *DGCR8*^{+/-} hESCs are also capable of differentiating spontaneously in the three germ layers.
- Monoallelic *DGCR8* disruption in hESCs does not always lead to 50% reduction in *DGCR8* mRNA expression in hESCs.
- *DGCR8* mRNA expression levels do not necessarily indicate protein levels or genetic background.
- While *DGCR8*^{+/-} hESCs partially recapitulate the position-dependent miRNA processing observed along the human C19MC, this phenomenon is distinct from the response seen in DROSHA knockdowns.

7. Summary

miRNAs regulate gene expression and influence biological processes (54). The Microprocessor complex – composed of DGCR8 and DROSHA- is essential for the first step of miRNA processing, thus serving as a highly relevant component in miRNA regulation (70). Systemic deletion of DGCR8 is lethal with an early arrest in development, while haploinsufficiency is present in a congenital disease, DGS (6,9). To date there is no other work studying the pluripotency and the differentiability capabilities of DGCR8^{+/-} hESCs, or the consequences of reduced DGCR8 levels in miRNA processing. This dissertation presents the establishment and characterization of a DGCR8 hemizygous hESC line. We applied a CRISPR-based knock-in/knock-out NHEJ approach with two tandem selection markers (GFP and puromycin resistance). Although we were unable to detect knockouts, a single cell clone (HVRDe009-A-1) carried the insert at the right location in a monoallelic manner. Without selection, gradual loss of transgene expression was observed in the clonal progeny of HVRDe009-A-1. Sanger sequencing data provided evidence for the sustained monoallelic disruption. The parental HVRDe009-A-1 and four selected subclones maintained normal karyotype despite transfection, cloning and selection steps. Our results demonstrate that DGCR8 haploinsufficiency does not alter the pluripotency and spontaneous differentiation capacity of hESCs. It is hard to find research papers concerning DGCR8 expression levels in hemizygous cells. Based on our results, the expression profile of Microprocessor components on the mRNA level can be inconclusive: compared to the wild-type, the HRVDe009-A-1 cells display indistinguishable *DGCR8* mRNA levels. The protein levels, however, show 40-60% reduction among them. A recent study reported that in DROSHA knockdown hESCs, the processing of the C19MC cluster members shows a position-dependent profile. Interestingly, HVRDe009-A-1 cells did not show 100% penetrance of this phenotype in our experiments. This could be explained by a better local DGCR8 recruitment caused by ERH-binding; however, further studies are needed to uncover this phenomenon. In conclusion, the HVRDe009-A-1 cell line may be a good model to examine the functions of DGCR8 and the regulatory network of Microprocessor components and its role in disease.

8. References

1. Du Q, de la Morena MT, van Oers NSC. The Genetics and Epigenetics of 22q11.2 Deletion Syndrome. *Front Genet.* 2019;10:1365.
2. Morrow BE, McDonald-McGinn DM, Emanuel BS, Vermeesch JR, Scambler PJ. Molecular genetics of 22q11.2 deletion syndrome. *Am J Med Genet A.* 2018 Oct;176(10):2070–2081.
3. Fryer A. Monozygotic twins with 22q11 deletion and discordant phenotypes. *J Med Genet.* 1996 Feb;33(2):173.
4. Yamagishi H, Ishii C, Maeda J, Kojima Y, Matsuoka R, Kimura M, Takao A, Momma K, Matsuo N. Phenotypic discordance in monozygotic twins with 22q11.2 deletion. *Am J Med Genet.* 1998 Jul 24;78(4):319–321.
5. Cirillo A, Lioncino M, Maratea A, Passariello A, Fusco A, Fratta F, Monda E, Caiazza M, Signore G, Esposito A, Baban A, Versacci P, Putotto C, Marino B, Pignata C, Cirillo E, Giardino G, Sarubbi B, Limongelli G, Russo MG. Clinical Manifestations of 22q11.2 Deletion Syndrome. *Heart Fail Clin.* 2022 Jan;18(1):155–164.
6. Meechan DW, Maynard TM, Tucker ES, LaMantia AS. Three phases of DiGeorge/22q11 deletion syndrome pathogenesis during brain development: patterning, proliferation, and mitochondrial functions of 22q11 genes. *Int J Dev Neurosci Off J Int Soc Dev Neurosci.* 2011 May;29(3):283–294.
7. Motahari Z, Moody SA, Maynard TM, LaMantia AS. In the line-up: deleted genes associated with DiGeorge/22q11.2 deletion syndrome: are they all suspects? *J Neurodev Disord.* 2019 Jun 7;11(1):7.
8. Kawahara Y. Human diseases caused by germline and somatic abnormalities in microRNA and microRNA-related genes. *Congenit Anom.* 2014 Feb;54(1):12–21.
9. Wang Y, Medvid R, Melton C, Jaenisch R, Blelloch R. DGCR8 is essential for microRNA biogenesis and silencing of embryonic stem cell self-renewal. *Nat Genet.* 2007 Mar;39(3):380–385.
10. Gierut JJ, Jacks TE, Haigis KM. Strategies to achieve conditional gene mutation in mice. *Cold Spring Harb Protoc.* 2014 Apr 1;2014(4):339–349.
11. Chapnik E, Sasson V, Blelloch R, Hornstein E. Dgcr8 controls neural crest cells survival in cardiovascular development. *Dev Biol.* 2012 Feb 1;362(1):50–56.
12. Rao PK, Toyama Y, Chiang HR, Gupta S, Bauer M, Medvid R, Reinhardt F, Liao R, Krieger M, Jaenisch R, Lodish HF, Blelloch R. Loss of cardiac microRNA-mediated regulation leads to dilated cardiomyopathy and heart failure. *Circ Res.* 2009 Sep 11;105(6):585–594.

13. Chen X, Wang L, Huang R, Qiu H, Wang P, Wu D, Zhu Y, Ming J, Wang Y, Wang J, Na J. Dgcr8 deletion in the primitive heart uncovered novel microRNA regulating the balance of cardiac-vascular gene program. *Protein Cell*. 2019 May;10(5):327–346.
14. Brandl A, Daum P, Brenner S, Schulz SR, Yap DYH, Bösl MR, Wittmann J, Schuh W, Jäck HM. The microprocessor component, DGCR8, is essential for early B-cell development in mice. *Eur J Immunol*. 2016 Dec;46(12):2710–2718.
15. Killy B, Bodendorfer B, Mages J, Ritter K, Schreiber J, Hölscher C, Pracht K, Ekici A, Jäck HM, Lang R. DGCR8 deficiency impairs macrophage growth and unleashes the interferon response to mycobacteria. *Life Sci Alliance*. 2021 Jun;4(6):e202000810.
16. Paylor R, McIlwain KL, McAninch R, Nellis A, Yuva-Paylor LA, Baldini A, Lindsay EA. Mice deleted for the DiGeorge/velocardiofacial syndrome region show abnormal sensorimotor gating and learning and memory impairments. *Hum Mol Genet*. 2001 Nov 1;10(23):2645–2650.
17. Stark KL, Xu B, Bagchi A, Lai WS, Liu H, Hsu R, Wan X, Pavlidis P, Mills AA, Karayiorgou M, Gogos JA. Altered brain microRNA biogenesis contributes to phenotypic deficits in a 22q11-deletion mouse model. *Nat Genet*. 2008 Jun;40(6):751–760.
18. Fénelon K, Xu B, Lai CS, Mukai J, Markx S, Stark KL, Hsu PK, Gan WB, Fischbach GD, MacDermott AB, Karayiorgou M, Gogos JA. The pattern of cortical dysfunction in a mouse model of a schizophrenia-related microdeletion. *J Neurosci Off J Soc Neurosci*. 2013 Sep 11;33(37):14825–14839.
19. Fénelon K, Mukai J, Xu B, Hsu PK, Drew LJ, Karayiorgou M, Fischbach GD, Macdermott AB, Gogos JA. Deficiency of Dgcr8, a gene disrupted by the 22q11.2 microdeletion, results in altered short-term plasticity in the prefrontal cortex. *Proc Natl Acad Sci U S A*. 2011 Mar 15;108(11):4447–4452.
20. Earls LR, Fricke RG, Yu J, Berry RB, Baldwin LT, Zakharenko SS. Age-dependent microRNA control of synaptic plasticity in 22q11 deletion syndrome and schizophrenia. *J Neurosci Off J Soc Neurosci*. 2012 Oct 10;32(41):14132–14144.
21. Amin H, Marinaro F, De Pietri Tonelli D, Berdondini L. Developmental excitatory-to-inhibitory GABA-polarity switch is disrupted in 22q11.2 deletion syndrome: a potential target for clinical therapeutics. *Sci Rep*. 2017 Nov 16;7(1):15752.
22. Deng L, Ren R, Liu Z, Song M, Li J, Wu Z, Ren X, Fu L, Li W, Zhang W, Guillen P, Izpisua Belmonte JC, Chan P, Qu J, Liu GH. Stabilizing heterochromatin by DGCR8 alleviates senescence and osteoarthritis. *Nat Commun*. 2019 Jul 26;10(1):3329.
23. Khan TA, Revah O, Gordon A, Yoon SJ, Krawisz AK, Goold C, Sun Y, Kim CH, Tian Y, Li MY, Schaepe JM, Ikeda K, Amin ND, Sakai N, Yazawa M, Kushan L,

- Nishino S, Porteus MH, Rapoport JL, Bernstein JA, O'Hara R, Bearden CE, Hallmayer JF, Huguenard JR, Geschwind DH, Dolmetsch RE, Paşca SP. Neuronal defects in a human cellular model of 22q11.2 deletion syndrome. *Nat Med*. 2020 Dec;26(12):1888–1898.
24. Macias S, Plass M, Stajuda A, Michlewski G, Eyraş E, Cáceres JF. DGCR8 HITS-CLIP reveals novel functions for the Microprocessor. *Nat Struct Mol Biol*. 2012 Aug;19(8):760–766.
 25. Macias S, Cordiner RA, Gautier P, Plass M, Cáceres JF. DGCR8 Acts as an Adaptor for the Exosome Complex to Degrade Double-Stranded Structured RNAs. *Mol Cell*. 2015 Dec 17;60(6):873–885.
 26. Yi R, Pasolli HA, Landthaler M, Hafner M, Ojo T, Sheridan R, Sander C, O'Carroll D, Stoffel M, Tuschl T, Fuchs E. DGCR8-dependent microRNA biogenesis is essential for skin development. *Proc Natl Acad Sci U S A*. 2009 Jan 13;106(2):498–502.
 27. Calses PC, Dhillon KK, Tucker N, Chi Y, Huang JW, Kawasumi M, Nghiem P, Wang Y, Clurman BE, Jacquemont C, Gafken PR, Sugawara K, Saijo M, Taniguchi T. DGCR8 Mediates Repair of UV-Induced DNA Damage Independently of RNA Processing. *Cell Rep*. 2017 Apr 4;19(1):162–174.
 28. Hang Q, Zeng L, Wang L, Nie L, Yao F, Teng H, Deng Y, Yap S, Sun Y, Frank SJ, Chen J, Ma L. Non-canonical function of DGCR8 in DNA double-strand break repair signaling and tumor radioresistance. *Nat Commun*. 2021 Jun 29;12(1):4033.
 29. Shefer K, Sperling J, Sperling R. The Supraspliceosome - A Multi-Task Machine for Regulated Pre-mRNA Processing in the Cell Nucleus. *Comput Struct Biotechnol J*. 2014 Sep;11(19):113–122.
 30. Shiohama A, Sasaki T, Noda S, Minoshima S, Shimizu N. Nucleolar localization of DGCR8 and identification of eleven DGCR8-associated proteins. *Exp Cell Res*. 2007 Dec 10;313(20):4196–4207.
 31. Kataoka N, Fujita M, Ohno M. Functional association of the Microprocessor complex with the spliceosome. *Mol Cell Biol*. 2009 Jun;29(12):3243–3254.
 32. Agranat-Tamir L, Shomron N, Sperling J, Sperling R. Interplay between pre-mRNA splicing and microRNA biogenesis within the supraspliceosome. *Nucleic Acids Res*. 2014 Apr;42(7):4640–4651.
 33. Salomonis N, Schlieve CR, Pereira L, Wahlquist C, Colas A, Zambon AC, Vranizan K, Spindler MJ, Pico AR, Cline MS, Clark TA, Williams A, Blume JE, Samal E, Mercola M, Merrill BJ, Conklin BR. Alternative splicing regulates mouse embryonic stem cell pluripotency and differentiation. *Proc Natl Acad Sci U S A*. 2010 Jun 8;107(23):10514–10519.

34. Cirera-Salinas D, Yu J, Bodak M, Ngondo RP, Herbert KM, Ciaudo C. Noncanonical function of DGCR8 controls mESC exit from pluripotency. *J Cell Biol.* 2017 Feb;216(2):355–366.
35. Marinaro F, Marzi MJ, Hoffmann N, Amin H, Pelizzoli R, Niola F, Nicassio F, De Pietri Tonelli D. MicroRNA-independent functions of DGCR8 are essential for neocortical development and TBR1 expression. *EMBO Rep.* 2017 Apr;18(4):603–618.
36. Heras SR, Macias S, Plass M, Fernandez N, Cano D, Eyraas E, Garcia-Perez JL, Cáceres JF. The Microprocessor controls the activity of mammalian retrotransposons. *Nat Struct Mol Biol.* 2013 Oct;20(10):1173–1181.
37. Bundo M, Toyoshima M, Okada Y, Akamatsu W, Ueda J, Nemoto-Miyauchi T, Sunaga F, Toritsuka M, Ikawa D, Kakita A, Kato M, Kasai K, Kishimoto T, Nawa H, Okano H, Yoshikawa T, Kato T, Iwamoto K. Increased L1 retrotransposition in the neuronal genome in schizophrenia. *Neuron.* 2014 Jan 22;81(2):306–313.
38. Witteveldt J, Ivens A, Macias S. Inhibition of Microprocessor Function during the Activation of the Type I Interferon Response. *Cell Rep.* 2018 Jun 12;23(11):3275–3285.
39. Faulkner GJ, Billon V. L1 retrotransposition in the soma: a field jumping ahead. *Mob DNA.* 2018;9:22.
40. Guffanti G, Gaudi S, Klengel T, Fallon JH, Mangalam H, Madduri R, Rodriguez A, DeCrescenzo P, Glovienka E, Sobell J, Klengel C, Pato M, Ressler KJ, Pato C, Macciardi F. LINE1 insertions as a genomic risk factor for schizophrenia: Preliminary evidence from an affected family. *Am J Med Genet Part B Neuropsychiatr Genet Off Publ Int Soc Psychiatr Genet.* 2016 Jun;171(4):534–545.
41. Terry DM, Devine SE. Aberrantly High Levels of Somatic LINE-1 Expression and Retrotransposition in Human Neurological Disorders. *Front Genet.* 2019;10:1244.
42. Reiner BC, Doyle GA, Weller AE, Levinson RN, Rao AM, Davila Perea E, Namoglu E, Pigeon A, Arauco-Shapiro G, Weickert CS, Turecki G, Crist RC, Berrettini WH. Inherited L1 Retrotransposon Insertions Associated With Risk for Schizophrenia and Bipolar Disorder. *Schizophr Bull Open.* 2021 Jan;2(1):sgab031.
43. Liu S, Du T, Liu Z, Shen Y, Xiu J, Xu Q. Inverse changes in L1 retrotransposons between blood and brain in major depressive disorder. *Sci Rep.* 2016 Nov 22;6:37530.
44. Zhu X, Zhou B, Pattni R, Gleason K, Tan C, Kalinowski A, Sloan S, Fiston-Lavier AS, Mariani J, Petrov D, Barres BA, Duncan L, Abyzov A, Vogel H, Brain Somatic Mosaicism Network, Moran JV, Vaccarino FM, Tamminga CA, Levinson DF, Urban AE. Machine learning reveals bilateral distribution of somatic L1 insertions in human neurons and glia. *Nat Neurosci.* 2021 Feb;24(2):186–196.

45. Cuarenta A, Kigar SL, Henion IC, Karls KE, Chang L, Bakshi VP, Auger AP. Early life stress increases Line1 within the developing brain in a sex-dependent manner. *Brain Res.* 2020 Dec 1;1748:147123.
46. Triboulet R, Chang HM, Lapierre RJ, Gregory RI. Post-transcriptional control of DGCR8 expression by the Microprocessor. *RNA N Y N.* 2009 Jun;15(6):1005–1011.
47. Han J, Pedersen JS, Kwon SC, Belair CD, Kim YK, Yeom KH, Yang WY, Haussler D, Blelloch R, Kim VN. Posttranscriptional crossregulation between Drosha and DGCR8. *Cell.* 2009 Jan 9;136(1):75–84.
48. Cui Y, Lyu X, Ding L, Ke L, Yang D, Pirouz M, Qi Y, Ong J, Gao G, Du P, Gregory RI. Global miRNA dosage control of embryonic germ layer specification. *Nature.* 2021 May;593(7860):602–606.
49. Lee D, Nam JW, Shin C. DROSHA targets its own transcript to modulate alternative splicing. *RNA N Y N.* 2017 Jul;23(7):1035–1047.
50. Link S, Grund SE, Diederichs S. Alternative splicing affects the subcellular localization of Drosha. *Nucleic Acids Res.* 2016 Jun 20;44(11):5330–5343.
51. Wang Y, Luo J, Zhang H, Lu J. microRNAs in the Same Clusters Evolve to Coordinately Regulate Functionally Related Genes. *Mol Biol Evol.* 2016 Sep;33(9):2232–2247.
52. Baek D, Villén J, Shin C, Camargo FD, Gygi SP, Bartel DP. The impact of microRNAs on protein output. *Nature.* 2008 Sep 4;455(7209):64–71.
53. Guo H, Ingolia NT, Weissman JS, Bartel DP. Mammalian microRNAs predominantly act to decrease target mRNA levels. *Nature.* 2010 Aug 12;466(7308):835–840.
54. Bartel DP. MicroRNAs: target recognition and regulatory functions. *Cell.* 2009 Jan 23;136(2):215–233.
55. Cherone JM, Jorgji V, Burge CB. Cotargeting among microRNAs in the brain. *Genome Res.* 2019 Nov;29(11):1791–1804.
56. Doench JG, Sharp PA. Specificity of microRNA target selection in translational repression. *Genes Dev.* 2004 Mar 1;18(5):504–511.
57. Grimson A, Farh KKH, Johnston WK, Garrett-Engele P, Lim LP, Bartel DP. MicroRNA targeting specificity in mammals: determinants beyond seed pairing. *Mol Cell.* 2007 Jul 6;27(1):91–105.
58. Hon LS, Zhang Z. The roles of binding site arrangement and combinatorial targeting in microRNA repression of gene expression. *Genome Biol.* 2007;8(8):R166.

59. Saetrom P, Heale BSE, Snøve O, Aagaard L, Alluin J, Rossi JJ. Distance constraints between microRNA target sites dictate efficacy and cooperativity. *Nucleic Acids Res.* 2007;35(7):2333–2342.
60. Whipple AJ, Breton-Provencher V, Jacobs HN, Chitta UK, Sur M, Sharp PA. Imprinted Maternally Expressed microRNAs Antagonize Paternally Driven Gene Programs in Neurons. *Mol Cell.* 2020 Apr 2;78(1):85-95.e8.
61. Cantini L, Bertoli G, Cava C, Dubois T, Zinovyev A, Caselle M, Castiglioni I, Barillot E, Martignetti L. Identification of microRNA clusters cooperatively acting on epithelial to mesenchymal transition in triple negative breast cancer. *Nucleic Acids Res.* 2019 Mar 18;47(5):2205–15.
62. Jin W, Mulas F, Gaertner B, Sui Y, Wang J, Matta I, Zeng C, Vinckier N, Wang A, Nguyen-Ngoc KV, Chiou J, Kaestner KH, Frazer KA, Carrano AC, Shih HP, Sander M. A Network of microRNAs Acts to Promote Cell Cycle Exit and Differentiation of Human Pancreatic Endocrine Cells. *iScience.* 2019 Nov 22;21:681–694.
63. Vishnoi A, Rani S. miRNA Biogenesis and Regulation of Diseases: An Updated Overview. *Methods Mol Biol Clifton NJ.* 2023;2595:1–12.
64. Nguyen TPN, Kumar M, Fedele E, Bonanno G, Bonifacino T. MicroRNA Alteration, Application as Biomarkers, and Therapeutic Approaches in Neurodegenerative Diseases. *Int J Mol Sci.* 2022 Apr 25;23(9):4718.
65. Vaghf A, Khansarinejad B, Ghaznavi-Rad E, Mondanizadeh M. The role of microRNAs in diseases and related signaling pathways. *Mol Biol Rep.* 2022 Jul;49(7):6789–6801.
66. Bartel DP. Metazoan MicroRNAs. *Cell.* 2018 Mar 22;173(1):20–51.
67. Treiber T, Treiber N, Meister G. Regulation of microRNA biogenesis and its crosstalk with other cellular pathways. *Nat Rev Mol Cell Biol.* 2019 Jan;20(1):5–20.
68. Suzuki HI, Young RA, Sharp PA. Super-Enhancer-Mediated RNA Processing Revealed by Integrative MicroRNA Network Analysis. *Cell.* 2017 Mar 9;168(6):1000-1014.e15.
69. Kim YK, Kim B, Kim VN. Re-evaluation of the roles of DROSHA, Exportin 5, and DICER in microRNA biogenesis. *Proc Natl Acad Sci U S A.* 2016 Mar 29;113(13):E1881-1889.
70. Gregory RI, Yan KP, Amuthan G, Chendrimada T, Doratotaj B, Cooch N, Shiekhattar R. The Microprocessor complex mediates the genesis of microRNAs. *Nature.* 2004 Nov 11;432(7014):235–240.

71. Liu Z, Wang J, Cheng H, Ke X, Sun L, Zhang QC, Wang HW. Cryo-EM Structure of Human Dicer and Its Complexes with a Pre-miRNA Substrate. *Cell*. 2018 May 17;173(5):1191-1203.e12.
72. Kawamata T, Tomari Y. Making RISC. *Trends Biochem Sci*. 2010 Jul;35(7):368–376.
73. Abdelfattah AM, Park C, Choi MY. Update on non-canonical microRNAs. *Biomol Concepts*. 2014 Aug;5(4):275–287.
74. Westholm JO, Lai EC. Mirtrons: microRNA biogenesis via splicing. *Biochimie*. 2011 Nov;93(11):1897–1904.
75. Berezikov E, Chung WJ, Willis J, Cuppen E, Lai EC. Mammalian mirtron genes. *Mol Cell*. 2007 Oct 26;28(2):328–336.
76. Ruby JG, Jan CH, Bartel DP. Intronic microRNA precursors that bypass Drosha processing. *Nature*. 2007 Jul 5;448(7149):83–86.
77. Babiarz JE, Ruby JG, Wang Y, Bartel DP, Blelloch R. Mouse ES cells express endogenous shRNAs, siRNAs, and other Microprocessor-independent, Dicer-dependent small RNAs. *Genes Dev*. 2008 Oct 15;22(20):2773–2785.
78. Wajahat M, Bracken CP, Orang A. Emerging Functions for snoRNAs and snoRNA-Derived Fragments. *Int J Mol Sci*. 2021 Sep 22;22(19):10193.
79. Patterson DG, Roberts JT, King VM, Houserova D, Barnhill EC, Crucello A, Polska CJ, Brantley LW, Kaufman GC, Nguyen M, Santana MW, Schiller IA, Spicciani JS, Zapata AK, Miller MM, Sherman TD, Ma R, Zhao H, Arora R, Coley AB, Zeidan MM, Tan M, Xi Y, Borchert GM. Human snoRNA-93 is processed into a microRNA-like RNA that promotes breast cancer cell invasion. *NPJ Breast Cancer*. 2017;3:25.
80. Dupuis-Sandoval F, Poirier M, Scott MS. The emerging landscape of small nucleolar RNAs in cell biology. *Wiley Interdiscip Rev RNA*. 2015;6(4):381–397.
81. Li W, Saraiya AA, Wang CC. Gene regulation in *Giardia lamblia* involves a putative microRNA derived from a small nucleolar RNA. *PLoS Negl Trop Dis*. 2011 Oct;5(10):e1338.
82. Ender C, Krek A, Friedländer MR, Beitzinger M, Weinmann L, Chen W, Pfeffer S, Rajewsky N, Meister G. A human snoRNA with microRNA-like functions. *Mol Cell*. 2008 Nov 21;32(4):519–528.
83. Scott MS, Avolio F, Ono M, Lamond AI, Barton GJ. Human miRNA precursors with box H/ACA snoRNA features. *PLoS Comput Biol*. 2009 Sep;5(9):e1000507.
84. Taft RJ, Glazov EA, Lassmann T, Hayashizaki Y, Carninci P, Mattick JS. Small RNAs derived from snoRNAs. *RNA N Y N*. 2009 Jul;15(7):1233–1240.

85. Langenberger D, Çakir MV, Hoffmann S, Stadler PF. Dicer-processed small RNAs: rules and exceptions. *J Exp Zool B Mol Dev Evol.* 2013 Jan;320(1):35–46.
86. Yi T, Arthanari H, Akabayov B, Song H, Papadopoulos E, Qi HH, Jedrychowski M, Güttler T, Guo C, Luna RE, Gygi SP, Huang SA, Wagner G. eIF1A augments Ago2-mediated Dicer-independent miRNA biogenesis and RNA interference. *Nat Commun.* 2015 May 28;6:7194.
87. Herrera-Carrillo E, Berkhout B. Dicer-independent processing of small RNA duplexes: mechanistic insights and applications. *Nucleic Acids Res.* 2017 Oct 13;45(18):10369–10379.
88. Hertel J, Lindemeyer M, Missal K, Fried C, Tanzer A, Flamm C, Hofacker IL, Stadler PF, Students of Bioinformatics Computer Labs 2004 and 2005. The expansion of the metazoan microRNA repertoire. *BMC Genomics.* 2006 Feb 15;7:25.
89. Malnou EC, Umlauf D, Mouysset M, Cavallé J. Imprinted MicroRNA Gene Clusters in the Evolution, Development, and Functions of Mammalian Placenta. *Front Genet.* 2018;9:706.
90. Guo L, Zhao Y, Zhang H, Yang S, Chen F. Integrated evolutionary analysis of human miRNA gene clusters and families implicates evolutionary relationships. *Gene.* 2014 Jan 15;534(1):24–32.
91. Li R, Yao X, Zhou H, Jin P, Ma F. The Drosophila miR-959-962 Cluster Members Repress Toll Signaling to Regulate Antibacterial Defense during Bacterial Infection. *Int J Mol Sci.* 2021 Jan 17;22(2):886.
92. Kim YK, Yu J, Han TS, Park SY, Namkoong B, Kim DH, Hur K, Yoo MW, Lee HJ, Yang HK, Kim VN. Functional links between clustered microRNAs: suppression of cell-cycle inhibitors by microRNA clusters in gastric cancer. *Nucleic Acids Res.* 2009 Apr;37(5):1672–1681.
93. Kotaki R, Higuchi H, Ogiya D, Katahira Y, Kurosaki N, Yukihiro N, Ogata J, Yamamoto H, Mohamad Alba S, Azhim A, Kitajima T, Inoue S, Morishita K, Ono K, Koyama-Nasu R, Kotani A. Imbalanced expression of polycistronic miRNA in acute myeloid leukemia. *Int J Hematol.* 2017 Dec;106(6):811–819.
94. Pratt ZL, Kuzembayeva M, Sengupta S, Sugden B. The microRNAs of Epstein-Barr Virus are expressed at dramatically differing levels among cell lines. *Virology.* 2009 Apr 10;386(2):387–397.
95. Ryazansky SS, Gvozdev VA, Berezhikov E. Evidence for post-transcriptional regulation of clustered microRNAs in Drosophila. *BMC Genomics.* 2011 Jul 19;12:371.

96. Fang W, Bartel DP. The Menu of Features that Define Primary MicroRNAs and Enable De Novo Design of MicroRNA Genes. *Mol Cell*. 2015 Oct 1;60(1):131–145.
97. Feederle R, Haar J, Bernhardt K, Linnstaedt SD, Bannert H, Lips H, Cullen BR, Delecluse HJ. The members of an Epstein-Barr virus microRNA cluster cooperate to transform B lymphocytes. *J Virol*. 2011 Oct;85(19):9801–9810.
98. Hutter K, Lohmüller M, Jukic A, Eichin F, Avci S, Labi V, Szabo TG, Hoser SM, Hüttenhofer A, Villunger A, Herzog S. SAFB2 Enables the Processing of Suboptimal Stem-Loop Structures in Clustered Primary miRNA Transcripts. *Mol Cell*. 2020 Jun 4;78(5):876-889.e6.
99. Shang R, Baek SC, Kim K, Kim B, Kim VN, Lai EC. Genomic Clustering Facilitates Nuclear Processing of Suboptimal Pri-miRNA Loci. *Mol Cell*. 2020 Apr 16;78(2):303-316.e4.
100. Vilimova M, Contrant M, Randrianjafy R, Dumas P, Elbasani E, Ojala PM, Pfeffer S, Fender A. Cis regulation within a cluster of viral microRNAs. *Nucleic Acids Res*. 2021 Sep 27;49(17):10018–10033.
101. Fang W, Bartel DP. MicroRNA Clustering Assists Processing of Suboptimal MicroRNA Hairpins through the Action of the ERH Protein. *Mol Cell*. 2020 Apr 16;78(2):289-302.e6.
102. Li S, Wang L, Fu B, Berman MA, Diallo A, Dorf ME. TRIM65 regulates microRNA activity by ubiquitination of TNRC6. *Proc Natl Acad Sci U S A*. 2014 May 13;111(19):6970–6975.
103. Kavanaugh G, Zhao R, Guo Y, Mohni KN, Glick G, Lacy ME, Hutson MS, Ascano M, Cortez D. Enhancer of Rudimentary Homolog Affects the Replication Stress Response through Regulation of RNA Processing. *Mol Cell Biol*. 2015 Sep 1;35(17):2979–2990.
104. Liz J, Portela A, Soler M, Gómez A, Ling H, Michlewski G, Calin GA, Guil S, Esteller M. Regulation of pri-miRNA processing by a long noncoding RNA transcribed from an ultraconserved region. *Mol Cell*. 2014 Jul 3;55(1):138–147.
105. Xiao L, Wu J, Wang JY, Chung HK, Kalakonda S, Rao JN, Gorospe M, Wang JY. Long Noncoding RNA uc.173 Promotes Renewal of the Intestinal Mucosa by Inducing Degradation of MicroRNA 195. *Gastroenterology*. 2018 Feb;154(3):599–611.
106. Han K, Wang FW, Cao CH, Ling H, Chen JW, Chen RX, Feng ZH, Luo J, Jin XH, Duan JL, Li SM, Ma NF, Yun JP, Guan XY, Pan ZZ, Lan P, Xu RH, Xie D. CircLONP2 enhances colorectal carcinoma invasion and metastasis through modulating the maturation and exosomal dissemination of microRNA-17. *Mol Cancer*. 2020 Mar 18;19(1):60.

107. Michlewski G, Guil S, Semple CA, Cáceres JF. Posttranscriptional regulation of miRNAs harboring conserved terminal loops. *Mol Cell*. 2008 Nov 7;32(3):383–393.
108. Kooshapur H, Choudhury NR, Simon B, Mühlbauer M, Jussupow A, Fernandez N, Jones AN, Dallmann A, Gabel F, Camilloni C, Michlewski G, Cáceres JF, Sattler M. Structural basis for terminal loop recognition and stimulation of pri-miRNA-18a processing by hnRNP A1. *Nat Commun*. 2018 Jun 26;9(1):2479.
109. Guil S, Cáceres JF. The multifunctional RNA-binding protein hnRNP A1 is required for processing of miR-18a. *Nat Struct Mol Biol*. 2007 Jul;14(7):591–596.
110. Soler M, Davalos V, Sánchez-Castillo A, Mora-Martinez C, Setién F, Siqueira E, Castro de Moura M, Esteller M, Guil S. The transcribed ultraconserved region uc.160+ enhances processing and A-to-I editing of the miR-376 cluster: hypermethylation improves glioma prognosis. *Mol Oncol*. 2022 Feb;16(3):648–664.
111. Sukoyan MA, Vatolin SY, Golubitsa AN, Zhelezova AI, Semenova LA, Serov OL. Embryonic stem cells derived from morulae, inner cell mass, and blastocysts of mink: comparisons of their pluripotencies. *Mol Reprod Dev*. 1993 Oct;36(2):148–158.
112. Thomson JA, Itskovitz-Eldor J, Shapiro SS, Waknitz MA, Swiergiel JJ, Marshall VS, Jones JM. Embryonic stem cell lines derived from human blastocysts. *Science*. 1998 Nov 6;282(5391):1145–1147.
113. Spangrude GJ, Heimfeld S, Weissman IL. Purification and characterization of mouse hematopoietic stem cells. *Science*. 1988 Jul 1;241(4861):58–62.
114. Costamagna D, Berardi E, Ceccarelli G, Sampaolesi M. Adult Stem Cells and Skeletal Muscle Regeneration. *Curr Gene Ther*. 2015;15(4):348–363.
115. Wobus AM, Boheler KR. Embryonic stem cells: prospects for developmental biology and cell therapy. *Physiol Rev*. 2005 Apr;85(2):635–678.
116. Hackett CH, Fortier LA. Embryonic stem cells and iPS cells: sources and characteristics. *Vet Clin North Am Equine Pract*. 2011 Aug;27(2):233–242.
117. Zakrzewski W, Dobrzyński M, Szymonowicz M, Rybak Z. Stem cells: past, present, and future. *Stem Cell Res Ther*. 2019 Feb 26;10(1):68.
118. Hasegawa K, Pomeroy JE, Pera MF. Current technology for the derivation of pluripotent stem cell lines from human embryos. *Cell Stem Cell*. 2010 Jun 4;6(6):521–531.
119. Devolder K. To be, or not to be? Are induced pluripotent stem cells potential babies, and does it matter? *EMBO Rep*. 2009 Dec;10(12):1285–1287.

120. Fadel HE. Developments in stem cell research and therapeutic cloning: Islamic ethical positions, a review. *Bioethics*. 2012 Mar;26(3):128–135.
121. Takahashi K, Tanabe K, Ohnuki M, Narita M, Ichisaka T, Tomoda K, Yamanaka S. Induction of pluripotent stem cells from adult human fibroblasts by defined factors. *Cell*. 2007 Nov 30;131(5):861–872.
122. Puri MC, Nagy A. Concise review: Embryonic stem cells versus induced pluripotent stem cells: the game is on. *Stem Cells Dayt Ohio*. 2012 Jan;30(1):10–14.
123. Rouhani FJ, Nik-Zainal S, Wuster A, Li Y, Conte N, Koike-Yusa H, Kumasaka N, Vallier L, Yusa K, Bradley A. Mutational History of a Human Cell Lineage from Somatic to Induced Pluripotent Stem Cells. *PLoS Genet*. 2016 Apr;12(4):e1005932.
124. Ji J, Ng SH, Sharma V, Neculai D, Hussein S, Sam M, Trinh Q, Church GM, McPherson JD, Nagy A, Batada NN. Elevated coding mutation rate during the reprogramming of human somatic cells into induced pluripotent stem cells. *Stem Cells Dayt Ohio*. 2012 Mar;30(3):435–440.
125. De Los Angeles A, Ferrari F, Xi R, Fujiwara Y, Benvenisty N, Deng H, Hochedlinger K, Jaenisch R, Lee S, Leitch HG, Lensch MW, Lujan E, Pei D, Rossant J, Wernig M, Park PJ, Daley GQ. Hallmarks of pluripotency. *Nature*. 2015 Sep 24;525(7570):469–478.
126. Boyer LA, Lee TI, Cole MF, Johnstone SE, Levine SS, Zucker JP, Guenther MG, Kumar RM, Murray HL, Jenner RG, Gifford DK, Melton DA, Jaenisch R, Young RA. Core transcriptional regulatory circuitry in human embryonic stem cells. *Cell*. 2005 Sep 23;122(6):947–956.
127. O'Connor MD, Kardel MD, Iosfina I, Youssef D, Lu M, Li MM, Vercauteren S, Nagy A, Eaves CJ. Alkaline phosphatase-positive colony formation is a sensitive, specific, and quantitative indicator of undifferentiated human embryonic stem cells. *Stem Cells Dayt Ohio*. 2008 May;26(5):1109–1116.
128. Choi SC, Choi JH, Park CY, Ahn CM, Hong SJ, Lim DS. Nanog regulates molecules involved in stemness and cell cycle-signaling pathway for maintenance of pluripotency of P19 embryonal carcinoma stem cells. *J Cell Physiol*. 2012 Nov;227(11):3678–3692.
129. Chambers I, Tomlinson SR. The transcriptional foundation of pluripotency. *Dev Camb Engl*. 2009 Jul;136(14):2311–2322.
130. Nelakanti RV, Kooreman NG, Wu JC. Teratoma formation: a tool for monitoring pluripotency in stem cell research. *Curr Protoc Stem Cell Biol*. 2015 Feb 2;32:4A.8.1-4A.8.17.
131. Höpfl G, Gassmann M, Desbaillets I. Differentiating embryonic stem cells into embryoid bodies. *Methods Mol Biol Clifton NJ*. 2004;254:79–98.

132. Kurosawa H. Methods for inducing embryoid body formation: in vitro differentiation system of embryonic stem cells. *J Biosci Bioeng.* 2007 May;103(5):389–398.
133. Burridge PW, Zambidis ET. Highly efficient directed differentiation of human induced pluripotent stem cells into cardiomyocytes. *Methods Mol Biol Clifton NJ.* 2013;997:149–161.
134. Takasato M, Er PX, Becroft M, Vanslambrouck JM, Stanley EG, Elefanty AG, Little MH. Directing human embryonic stem cell differentiation towards a renal lineage generates a self-organizing kidney. *Nat Cell Biol.* 2014 Jan;16(1):118–126.
135. Huang SXL, Islam MN, O’Neill J, Hu Z, Yang YG, Chen YW, Mumau M, Green MD, Vunjak-Novakovic G, Bhattacharya J, Snoeck HW. Efficient generation of lung and airway epithelial cells from human pluripotent stem cells. *Nat Biotechnol.* 2014 Jan;32(1):84–91.
136. Wichterle H, Lieberam I, Porter JA, Jessell TM. Directed differentiation of embryonic stem cells into motor neurons. *Cell.* 2002 Aug 9;110(3):385–397.
137. Spence JR, Mayhew CN, Rankin SA, Kuhar MF, Vallance JE, Tolle K, Hoskins EE, Kalinichenko VV, Wells SI, Zorn AM, Shroyer NF, Wells JM. Directed differentiation of human pluripotent stem cells into intestinal tissue in vitro. *Nature.* 2011 Feb 3;470(7332):105–109.
138. Oldershaw RA, Baxter MA, Lowe ET, Bates N, Grady LM, Soncin F, Brison DR, Hardingham TE, Kimber SJ. Directed differentiation of human embryonic stem cells toward chondrocytes. *Nat Biotechnol.* 2010 Nov;28(11):1187–1194.
139. Aronovich EL, McIvor RS, Hackett PB. The Sleeping Beauty transposon system: a non-viral vector for gene therapy. *Hum Mol Genet.* 2011 Apr 15;20(R1):R14-20.
140. Rapti K, Stillitano F, Karakikes I, Nonnenmacher M, Weber T, Hulot JS, Hajjar RJ. Effectiveness of gene delivery systems for pluripotent and differentiated cells. *Mol Ther Methods Clin Dev.* 2015;2:14067.
141. Hoffmann D, Schott JW, Geis FK, Lange L, Müller FJ, Lenz D, Zychlinski D, Steinemann D, Morgan M, Moritz T, Schambach A. Detailed comparison of retroviral vectors and promoter configurations for stable and high transgene expression in human induced pluripotent stem cells. *Gene Ther.* 2017 May;24(5):298–307.
142. Naujok O, Diekmann U, Elsner M. Gene Transfer into Pluripotent Stem Cells via Lentiviral Transduction. *Methods Mol Biol Clifton NJ.* 2016;1341:67–85.
143. Brokhman I, Pomp O, Fishman L, Tennenbaum T, Amit M, Itzkovitz-Eldor J, Goldstein RS. Genetic modification of human embryonic stem cells with adenoviral vectors: differences of infectability between lines and correlation of infectability with expression of the coxsackie and adenovirus receptor. *Stem Cells Dev.* 2009 Apr;18(3):447–456.

144. Sung LY, Chen CL, Lin SY, Li KC, Yeh CL, Chen GY, Lin CY, Hu YC. Efficient gene delivery into cell lines and stem cells using baculovirus. *Nat Protoc.* 2014 Aug;9(8):1882–1899.
145. Heyer WD, Ehmsen KT, Liu J. Regulation of homologous recombination in eukaryotes. *Annu Rev Genet.* 2010;44:113–139.
146. Koller BH, Hagemann LJ, Doetschman T, Hagaman JR, Huang S, Williams PJ, First NL, Maeda N, Smithies O. Germ-line transmission of a planned alteration made in a hypoxanthine phosphoribosyltransferase gene by homologous recombination in embryonic stem cells. *Proc Natl Acad Sci U S A.* 1989 Nov;86(22):8927–8931.
147. Maeder ML, Thibodeau-Beganny S, Osiak A, Wright DA, Anthony RM, Eichtinger M, Jiang T, Foley JE, Winfrey RJ, Townsend JA, Unger-Wallace E, Sander JD, Müller-Lerch F, Fu F, Pearlberg J, Göbel C, Dassie JP, Pruett-Miller SM, Porteus MH, Sgroi DC, Iafrate AJ, Dobbs D, McCray PB, Cathomen T, Voytas DF, Joung JK. Rapid “open-source” engineering of customized zinc-finger nucleases for highly efficient gene modification. *Mol Cell.* 2008 Jul 25;31(2):294–301.
148. Reyon D, Tsai SQ, Khayter C, Foden JA, Sander JD, Joung JK. FLASH assembly of TALENs for high-throughput genome editing. *Nat Biotechnol.* 2012 May;30(5):460–465.
149. Cong L, Ran FA, Cox D, Lin S, Barretto R, Habib N, Hsu PD, Wu X, Jiang W, Marraffini LA, Zhang F. Multiplex genome engineering using CRISPR/Cas systems. *Science.* 2013 Feb 15;339(6121):819–823.
150. Mali P, Yang L, Esvelt KM, Aach J, Guell M, DiCarlo JE, Norville JE, Church GM. RNA-guided human genome engineering via Cas9. *Science.* 2013 Feb 15;339(6121):823–826.
151. Mojica FJM, Díez-Villaseñor C, García-Martínez J, Almendros C. Short motif sequences determine the targets of the prokaryotic CRISPR defence system. *Microbiol Read Engl.* 2009 Mar;155(Pt 3):733–740.
152. Makarova KS, Wolf YI, Alkhnbashi OS, Costa F, Shah SA, Saunders SJ, Barrangou R, Brouns SJJ, Charpentier E, Haft DH, Horvath P, Moineau S, Mojica FJM, Terns RM, Terns MP, White MF, Yakunin AF, Garrett RA, van der Oost J, Backofen R, Koonin EV. An updated evolutionary classification of CRISPR-Cas systems. *Nat Rev Microbiol.* 2015 Nov;13(11):722–736.
153. Bhardwaj A, Nain V. TALENs-an indispensable tool in the era of CRISPR: a mini review. *J Genet Eng Biotechnol.* 2021 Aug 21;19(1):125.
154. Kim D, Kim JS. DIG-seq: a genome-wide CRISPR off-target profiling method using chromatin DNA. *Genome Res.* 2018 Dec;28(12):1894–1900.

155. Guilinger JP, Thompson DB, Liu DR. Fusion of catalytically inactive Cas9 to FokI nuclease improves the specificity of genome modification. *Nat Biotechnol.* 2014 Jun;32(6):577–582.
156. Tsai SQ, Wyvekens N, Khayter C, Foden JA, Thapar V, Reyon D, Goodwin MJ, Aryee MJ, Joung JK. Dimeric CRISPR RNA-guided FokI nucleases for highly specific genome editing. *Nat Biotechnol.* 2014 Jun;32(6):569–576.
157. Ran FA, Hsu PD, Lin CY, Gootenberg JS, Konermann S, Trevino AE, Scott DA, Inoue A, Matoba S, Zhang Y, Zhang F. Double nicking by RNA-guided CRISPR Cas9 for enhanced genome editing specificity. *Cell.* 2013 Sep 12;154(6):1380–1389.
158. Kim YH, Kim N, Okafor I, Choi S, Min S, Lee J, Bae SM, Choi K, Choi J, Harihar V, Kim Y, Kim JS, Kleinstiver BP, Lee JK, Ha T, Kim HH. Sniper2L is a high-fidelity Cas9 variant with high activity. *Nat Chem Biol.* 2023 Aug;19(8):972–980.
159. Moore JK, Haber JE. Cell cycle and genetic requirements of two pathways of nonhomologous end-joining repair of double-strand breaks in *Saccharomyces cerevisiae*. *Mol Cell Biol.* 1996 May;16(5):2164–2173.
160. Rodgers K, McVey M. Error-Prone Repair of DNA Double-Strand Breaks. *J Cell Physiol.* 2016 Jan;231(1):15–24.
161. Symington LS, Gautier J. Double-strand break end resection and repair pathway choice. *Annu Rev Genet.* 2011;45:247–271.
162. Gu J, Lieber MR. Mechanistic flexibility as a conserved theme across 3 billion years of nonhomologous DNA end-joining. *Genes Dev.* 2008 Feb 15;22(4):411–415.
163. San Filippo J, Sung P, Klein H. Mechanism of eukaryotic homologous recombination. *Annu Rev Biochem.* 2008;77:229–257.
164. Yang D, Scavuzzo MA, Chmielowiec J, Sharp R, Bajic A, Borowiak M. Enrichment of G2/M cell cycle phase in human pluripotent stem cells enhances HDR-mediated gene repair with customizable endonucleases. *Sci Rep.* 2016 Feb 18;6:21264.
165. He X, Tan C, Wang F, Wang Y, Zhou R, Cui D, You W, Zhao H, Ren J, Feng B. Knock-in of large reporter genes in human cells via CRISPR/Cas9-induced homology-dependent and independent DNA repair. *Nucleic Acids Res.* 2016 May 19;44(9):e85.
166. Cox DBT, Platt RJ, Zhang F. Therapeutic genome editing: prospects and challenges. *Nat Med.* 2015 Feb;21(2):121–131.
167. Capecchi MR. Altering the genome by homologous recombination. *Science.* 1989 Jun 16;244(4910):1288–1292.

168. Thomas KR, Capecchi MR. Targeting of genes to specific sites in the mammalian genome. *Cold Spring Harb Symp Quant Biol.* 1986;51 Pt 2:1101–1113.
169. Thomas KR, Folger KR, Capecchi MR. High frequency targeting of genes to specific sites in the mammalian genome. *Cell.* 1986 Feb 14;44(3):419–428.
170. Capecchi MR. Gene targeting in mice: functional analysis of the mammalian genome for the twenty-first century. *Nat Rev Genet.* 2005 Jun;6(6):507–512.
171. Yeh CD, Richardson CD, Corn JE. Advances in genome editing through control of DNA repair pathways. *Nat Cell Biol.* 2019 Dec;21(12):1468–1478.
172. Miyaoka Y, Berman JR, Cooper SB, Mayerl SJ, Chan AH, Zhang B, Karlin-Neumann GA, Conklin BR. Systematic quantification of HDR and NHEJ reveals effects of locus, nuclease, and cell type on genome-editing. *Sci Rep.* 2016 Mar 31;6:23549.
173. Shi Y, Inoue H, Wu JC, Yamanaka S. Induced pluripotent stem cell technology: a decade of progress. *Nat Rev Drug Discov.* 2017 Feb;16(2):115–130.
174. Levy N. The use of animal as models: ethical considerations. *Int J Stroke Off J Int Stroke Soc.* 2012 Jul;7(5):440–442.
175. MacDougall G, Brown LY, Kantor B, Chiba-Falek O. The Path to Progress Preclinical Studies of Age-Related Neurodegenerative Diseases: A Perspective on Rodent and hiPSC-Derived Models. *Mol Ther J Am Soc Gene Ther.* 2021 Mar 3;29(3):949–972.
176. van der Velden J, Asselbergs FW, Bakkens J, Batkai S, Bertrand L, Bezzina CR, Bot I, Brundel BJM, Carrier L, Chamuleau S, Ciccarelli M, Dawson D, Davidson SM, Dendorfer A, Duncker DJ, Eschenhagen T, Fabritz L, Falcão-Pires I, Ferdinandy P, Giacca M, Girao H, Gollmann-Tepeköylü C, Gyongyosi M, Guzik TJ, Hamdani N, Heymans S, Hilfiker A, Hilfiker-Kleiner D, Hoekstra AG, Hulot JS, Kuster DWD, van Laake LW, Lecour S, Leiner T, Linke WA, Lumens J, Lutgens E, Madonna R, Maegdefessel L, Mayr M, van der Meer P, Passier R, Perbellini F, Perrino C, Pesce M, Priori S, Remme CA, Rosenhahn B, Schotten U, Schulz R, Sipido KR, Sluijter JPG, van Steenbeek F, Steffens S, Terracciano CM, Tocchetti CG, Vlasman P, Yeung KK, Zacchigna S, Zwaagman D, Thum T. Animal models and animal-free innovations for cardiovascular research: current status and routes to be explored. Consensus document of the ESC Working Group on Myocardial Function and the ESC Working Group on Cellular Biology of the Heart. *Cardiovasc Res.* 2022 Dec 9;118(15):3016–3051.
177. Deng B. Mouse models and induced pluripotent stem cells in researching psychiatric disorders. *Stem Cell Investig.* 2017;4:62.
178. Kytälä A, Moraghebi R, Valensisi C, Kettunen J, Andrus C, Pasumarthy KK, Nakanishi M, Nishimura K, Ohtaka M, Weltner J, Van Handel B, Parkkonen O, Sinisalo J, Jalanko A, Hawkins RD, Woods NB, Otonkoski T, Trokovic R. Genetic

- Variability Overrides the Impact of Parental Cell Type and Determines iPSC Differentiation Potential. *Stem Cell Rep.* 2016 Feb 9;6(2):200–212.
179. Burrows CK, Banovich NE, Pavlovic BJ, Patterson K, Gallego Romero I, Pritchard JK, Gilad Y. Genetic Variation, Not Cell Type of Origin, Underlies the Majority of Identifiable Regulatory Differences in iPSCs. *PLoS Genet.* 2016 Jan;12(1):e1005793.
 180. Kilpinen H, Goncalves A, Leha A, Afzal V, Alasoo K, Ashford S, Bala S, Bensaddek D, Casale FP, Culley OJ, Danecek P, Faulconbridge A, Harrison PW, Kathuria A, McCarthy D, McCarthy SA, Meleckyte R, Memari Y, Moens N, Soares F, Mann A, Streeter I, Agu CA, Alderton A, Nelson R, Harper S, Patel M, White A, Patel SR, Clarke L, Halai R, Kirton CM, Kolb-Kokocinski A, Beales P, Birney E, Danovi D, Lamond AI, Ouwehand WH, Vallier L, Watt FM, Durbin R, Stegle O, Gaffney DJ. Common genetic variation drives molecular heterogeneity in human iPSCs. *Nature.* 2017 Jun 15;546(7658):370–375.
 181. Yumlu S, Stumm J, Bashir S, Dreyer AK, Lisowski P, Danner E, Kühn R. Gene editing and clonal isolation of human induced pluripotent stem cells using CRISPR/Cas9. *Methods San Diego Calif.* 2017 May 15;121–122:29–44.
 182. Chen KG, Mallon BS, Park K, Robey PG, McKay RDG, Gottesman MM, Zheng W. Pluripotent Stem Cell Platforms for Drug Discovery. *Trends Mol Med.* 2018 Sep;24(9):805–820.
 183. Uchimura T, Otomo J, Sato M, Sakurai H. A human iPS cell myogenic differentiation system permitting high-throughput drug screening. *Stem Cell Res.* 2017 Dec;25:98–106.
 184. Prondzynski M, Lemoine MD, Zech AT, Horváth A, Di Mauro V, Koivumäki JT, Kresin N, Busch J, Krause T, Krämer E, Schlossarek S, Spohn M, Friedrich FW, Münch J, Laufer SD, Redwood C, Volk AE, Hansen A, Mearini G, Catalucci D, Meyer C, Christ T, Patten M, Eschenhagen T, Carrier L. Disease modeling of a mutation in α -actinin 2 guides clinical therapy in hypertrophic cardiomyopathy. *EMBO Mol Med.* 2019 Dec;11(12):e11115.
 185. de Boer RA, Heymans S, Backs J, Carrier L, Coats AJS, Dimmeler S, Eschenhagen T, Filippatos G, Gepstein L, Hulot JS, Knöll R, Kupatt C, Linke WA, Seidman CE, Tocchetti CG, van der Velden J, Walsh R, Seferovic PM, Thum T. Targeted therapies in genetic dilated and hypertrophic cardiomyopathies: from molecular mechanisms to therapeutic targets. A position paper from the Heart Failure Association (HFA) and the Working Group on Myocardial Function of the European Society of Cardiology (ESC). *Eur J Heart Fail.* 2022 Mar;24(3):406–420.
 186. Zhu L, Sun C, Ren J, Wang G, Ma R, Sun L, Yang D, Gao S, Ning K, Wang Z, Chen X, Chen S, Zhu H, Gao Z, Xu J. Stress-induced precocious aging in PD-patient iPSC-derived NSCs may underlie the pathophysiology of Parkinson's disease. *Cell Death Dis.* 2019 Feb 4;10(2):105.

187. Bose A, Petsko GA, Studer L. Induced pluripotent stem cells: a tool for modeling Parkinson's disease. *Trends Neurosci.* 2022 Aug;45(8):608–620.
188. Mertens J, Herdy JR, Traxler L, Schafer ST, Schlachetzki JCM, Böhnke L, Reid DA, Lee H, Zangwill D, Fernandes DP, Agarwal RK, Lucciola R, Zhou-Yang L, Karbacher L, Edenhofer F, Stern S, Horvath S, Paquola ACM, Glass CK, Yuan SH, Ku M, Szücs A, Goldstein LSB, Galasko D, Gage FH. Age-dependent instability of mature neuronal fate in induced neurons from Alzheimer's patients. *Cell Stem Cell.* 2021 Sep 2;28(9):1533-1548.e6.
189. Okano H, Yasuda D, Fujimori K, Morimoto S, Takahashi S. Ropinirole, a New ALS Drug Candidate Developed Using iPSCs. *Trends Pharmacol Sci.* 2020 Feb;41(2):99–109.
190. Ito D, Morimoto S, Takahashi S, Okada K, Nakahara J, Okano H. Maiden voyage: induced pluripotent stem cell-based drug screening for amyotrophic lateral sclerosis. *Brain J Neurol.* 2023 Jan 5;146(1):13–19.
191. Doss MX, Sachinidis A. Current Challenges of iPSC-Based Disease Modeling and Therapeutic Implications. *Cells.* 2019 Apr 30;8(5):403.
192. Karbassi E, Fenix A, Marchiano S, Muraoka N, Nakamura K, Yang X, Murry CE. Cardiomyocyte maturation: advances in knowledge and implications for regenerative medicine. *Nat Rev Cardiol.* 2020 Jun;17(6):341–359.
193. Onódi Z, Visnovitz T, Kiss B, Hambalkó S, Koncz A, Ágg B, Váradi B, Tóth VÉ, Nagy RN, Gergely TG, Gergő D, Makkos A, Pelyhe C, Varga N, Reé D, Apáti Á, Leszek P, Kovács T, Nagy N, Ferdinandy P, Buzás EI, Görbe A, Giricz Z, Varga ZV. Systematic transcriptomic and phenotypic characterization of human and murine cardiac myocyte cell lines and primary cardiomyocytes reveals serious limitations and low resemblances to adult cardiac phenotype. *J Mol Cell Cardiol.* 2022 Apr;165:19–30.
194. Doss MX, Di Diego JM, Goodrow RJ, Wu Y, Cordeiro JM, Nesterenko VV, Barajas-Martínez H, Hu D, Urrutia J, Desai M, Treat JA, Sachinidis A, Antzelevitch C. Maximum diastolic potential of human induced pluripotent stem cell-derived cardiomyocytes depends critically on I(Kr). *PloS One.* 2012;7(7):e40288.
195. Vera E, Bosco N, Studer L. Generating Late-Onset Human iPSC-Based Disease Models by Inducing Neuronal Age-Related Phenotypes through Telomerase Manipulation. *Cell Rep.* 2016 Oct 18;17(4):1184–1192.
196. Aversano S, Caiazza C, Caiazzo M. Induced pluripotent stem cell-derived and directly reprogrammed neurons to study neurodegenerative diseases: The impact of aging signatures. *Front Aging Neurosci.* 2022;14:1069482.
197. Lemme M, Ulmer BM, Lemoine MD, Zech ATL, Flenner F, Ravens U, Reichensperner H, Rol-Garcia M, Smith G, Hansen A, Christ T, Eschenhagen T.

- Atrial-like Engineered Heart Tissue: An In Vitro Model of the Human Atrium. *Stem Cell Rep.* 2018 Dec 11;11(6):1378–1390.
198. James EC, Tomaskovic-Crook E, Crook JM. Bioengineering Clinically Relevant Cardiomyocytes and Cardiac Tissues from Pluripotent Stem Cells. *Int J Mol Sci.* 2021 Mar 16;22(6):3005.
 199. Ng WH, Johnston EK, Tan JJ, Bliley JM, Feinberg AW, Stolz DB, Sun M, Wijesekara P, Hawkins F, Kotton DN, Ren X. Recapitulating human cardiopulmonary co-development using simultaneous multilineage differentiation of pluripotent stem cells. *eLife.* 2022 Jan 12;11:e67872.
 200. Zhang J, Klos M, Wilson GF, Herman AM, Lian X, Raval KK, Barron MR, Hou L, Soerens AG, Yu J, Palecek SP, Lyons GE, Thomson JA, Herron TJ, Jalife J, Kamp TJ. Extracellular matrix promotes highly efficient cardiac differentiation of human pluripotent stem cells: the matrix sandwich method. *Circ Res.* 2012 Oct 12;111(9):1125–1136.
 201. Yoshida S, Miyagawa S, Fukushima S, Kawamura T, Kashiyama N, Ohashi F, Toyofuku T, Toda K, Sawa Y. Maturation of Human Induced Pluripotent Stem Cell-Derived Cardiomyocytes by Soluble Factors from Human Mesenchymal Stem Cells. *Mol Ther J Am Soc Gene Ther.* 2018 Nov 7;26(11):2681–2695.
 202. Parikh SS, Blackwell DJ, Gomez-Hurtado N, Frisk M, Wang L, Kim K, Dahl CP, Fiane A, Tønnessen T, Kryshthal DO, Louch WE, Knollmann BC. Thyroid and Glucocorticoid Hormones Promote Functional T-Tubule Development in Human-Induced Pluripotent Stem Cell-Derived Cardiomyocytes. *Circ Res.* 2017 Dec 8;121(12):1323–1330.
 203. Tani H, Tohyama S. Human Engineered Heart Tissue Models for Disease Modeling and Drug Discovery. *Front Cell Dev Biol.* 2022;10:855763.
 204. Tálas A, Kulcsár PI, Weinhardt N, Borsy A, Tóth E, Szebényi K, Krausz SL, Huszár K, Vida I, Sturm Á, Gordos B, Hoffmann OI, Bencsura P, Nyeste A, Ligeti Z, Fodor E, Welker E. A convenient method to pre-screen candidate guide RNAs for CRISPR/Cas9 gene editing by NHEJ-mediated integration of a “self-cleaving” GFP-expression plasmid. *DNA Res Int J Rapid Publ Rep Genes Genomes.* 2017 Dec 1;24(6):609–621.
 205. Reé D, Borsy A, Fóthi Á, Orbán TI, Várady G, Erdei Z, Sarkadi B, Réthelyi J, Varga N, Apáti Á. Establishing a human embryonic stem cell clone with a heterozygous mutation in the DGCR8 gene. *Stem Cell Res.* 2020 Dec 22;50:102134.
 206. Reé D, Fóthi Á, Varga N, Kolacsek O, Orbán TI, Apáti Á. Partial Disturbance of Microprocessor Function in Human Stem Cells Carrying a Heterozygous Mutation in the DGCR8 Gene. *Genes.* 2022 Oct 23;13(11):1925.
 207. Han J, Lee Y, Yeom KH, Kim YK, Jin H, Kim VN. The Drosha-DGCR8 complex in primary microRNA processing. *Genes Dev.* 2004 Dec 15;18(24):3016–3027.

208. Fóthi Á, Biró O, Erdei Z, Apáti Á, Orbán TI. Tissue-specific and transcription-dependent mechanisms regulate primary microRNA processing efficiency of the human chromosome 19 MicroRNA cluster. *RNA Biol.* 2021 Aug;18(8):1170–1180.
209. Nguyen TA, Jo MH, Choi YG, Park J, Kwon SC, Hohng S, Kim VN, Woo JS. Functional Anatomy of the Human Microprocessor. *Cell.* 2015 Jun 4;161(6):1374–1387.
210. McDonald-McGinn DM, Sullivan KE, Marino B, Philip N, Swillen A, Vorstman JAS, Zackai EH, Emanuel BS, Vermeesch JR, Morrow BE, Scambler PJ, Bassett AS. 22q11.2 deletion syndrome. *Nat Rev Dis Primer.* 2015 Nov 19;1:15071.
211. Schnerch A, Cerdan C, Bhatia M. Distinguishing between mouse and human pluripotent stem cell regulation: the best laid plans of mice and men. *Stem Cells Dayt Ohio.* 2010 Mar 31;28(3):419–430.
212. Ginis I, Luo Y, Miura T, Thies S, Brandenberger R, Gerecht-Nir S, Amit M, Hoke A, Carpenter MK, Itskovitz-Eldor J, Rao MS. Differences between human and mouse embryonic stem cells. *Dev Biol.* 2004 May 15;269(2):360–380.
213. Maynard S, Swistowska AM, Lee JW, Liu Y, Liu ST, Da Cruz AB, Rao M, de Souza-Pinto NC, Zeng X, Bohr VA. Human embryonic stem cells have enhanced repair of multiple forms of DNA damage. *Stem Cells Dayt Ohio.* 2008 Sep;26(9):2266–2274.
214. Tomishima M. Conditioning pluripotent stem cell media with mouse embryonic fibroblasts (MEF-CM). In: *StemBook* [Internet]. Cambridge (MA): Harvard Stem Cell Institute; 2008 [cited 2023 May 22]. Available from: <http://www.ncbi.nlm.nih.gov/books/NBK133270/>
215. Baker DEC, Harrison NJ, Maltby E, Smith K, Moore HD, Shaw PJ, Heath PR, Holden H, Andrews PW. Adaptation to culture of human embryonic stem cells and oncogenesis in vivo. *Nat Biotechnol.* 2007 Feb;25(2):207–215.
216. Moon SH, Kim JS, Park SJ, Lim JJ, Lee HJ, Lee SM, Chung HM. Effect of chromosome instability on the maintenance and differentiation of human embryonic stem cells in vitro and in vivo. *Stem Cell Res.* 2011 Jan;6(1):50–59.
217. Momcilovic O, Knobloch L, Fornasaglio J, Varum S, Easley C, Schatten G. DNA damage responses in human induced pluripotent stem cells and embryonic stem cells. *PLoS One.* 2010 Oct 15;5(10):e13410.
218. Adams BR, Hawkins AJ, Povirk LF, Valerie K. ATM-independent, high-fidelity nonhomologous end joining predominates in human embryonic stem cells. *Aging.* 2010 Sep;2(9):582–596.
219. Eggenschwiler R, Loya K, Wu G, Sharma AD, Sgodda M, Zychlinski D, Herr C, Steinemann D, Teckman J, Bals R, Ott M, Schambach A, Schöler HR, Cantz T. Sustained knockdown of a disease-causing gene in patient-specific induced

- pluripotent stem cells using lentiviral vector-based gene therapy. *Stem Cells Transl Med.* 2013 Sep;2(9):641–654.
220. Larson JS, Yin M, Fischer JM, Stringer SL, Stringer JR. Expression and loss of alleles in cultured mouse embryonic fibroblasts and stem cells carrying allelic fluorescent protein genes. *BMC Mol Biol.* 2006 Oct 16;7:36.
 221. Schofield CM, Hsu R, Barker AJ, Gertz CC, Blelloch R, Ullian EM. Monoallelic deletion of the microRNA biogenesis gene *Dgcr8* produces deficits in the development of excitatory synaptic transmission in the prefrontal cortex. *Neural Develop.* 2011 Apr 5;6:11.
 222. Conrad T, Marsico A, Gehre M, Orom UA. Microprocessor activity controls differential miRNA biogenesis *In Vivo*. *Cell Rep.* 2014 Oct 23;9(2):542–554.
 223. Bellemer C, Bortolin-Cavaillé ML, Schmidt U, Jensen SMR, Kjems J, Bertrand E, Cavaillé J. Microprocessor dynamics and interactions at endogenous imprinted C19MC microRNA genes. *J Cell Sci.* 2012 Jun 1;125(Pt 11):2709–2720.
 224. Kwon SC, Jang H, Shen S, Baek SC, Kim K, Yang J, Kim J, Kim JS, Wang S, Shi Y, Li F, Kim VN. ERH facilitates microRNA maturation through the interaction with the N-terminus of DGCR8. *Nucleic Acids Res.* 2020 Nov 4;48(19):11097–11112.

9. Bibliography of the candidate's publication

9.1. Publications related to the PhD thesis

Reé D, Borsy A, Fóthi Á, Orbán TI, Várady G, Erdei Z, Sarkadi B, Réthelyi JM, Varga N, Apáti Á. Establishing a human embryonic stem cell clone with a heterozygous mutation in the DGCR8 gene. *Stem Cell Res.* 2020 Dec 22;50:102134.

Reé D, Fóthi Á, Varga N, Kolacsek O, Orbán TI, Apáti Á. Partial Disturbance of Microprocessor Function in Human Stem Cells Carrying a Heterozygous Mutation in the DGCR8 Gene. *Genes.* 2022 Oct 23;13(11):1925.

9.2. Other publications

Szabó E, Juhász F, Hathy E, Reé D, Homolya L, Erdei Z, Réthelyi JM, Apáti Á. Functional Comparison of Blood-Derived Human Neural Progenitor Cells. *Int J Mol Sci.* 2020 Nov 30;21(23):9118.

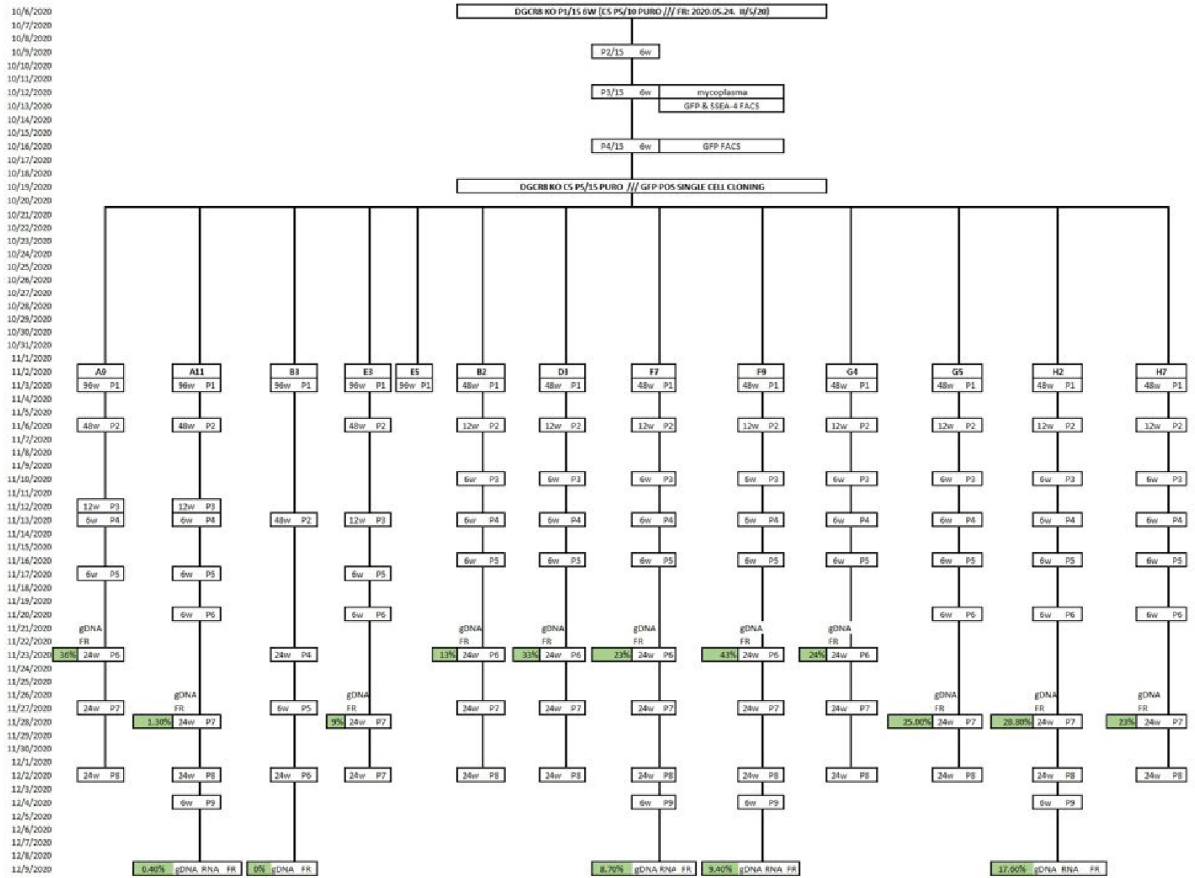
Szabó E, Reé D, Jezsó B, Vincze K, Földes G, Molnár AA, Réthelyi JM, Apáti Á. Generation of iPSC lines from peripheral blood mononuclear cells of identical twins both suffering from type 2 diabetes mellitus and one of them additionally diagnosed with atherosclerosis. *Stem Cell Res.* 2020 Dec;49:102051.

Onódi Z, Visnovitz T, Kiss B, Hambalkó S, Koncz A, Ágg B, Váradi B, Tóth VÉ, Nagy RN, Gergely TG, Gergő D, Makkos A, Pelyhe C, Varga N, Reé D, Apáti Á, Leszek P, Kovács T, Nagy N, Ferdinandy P, Buzás E, Görbe A, Giricz Z, Varga ZV. Systematic transcriptomic and phenotypic characterization of human and murine cardiac myocyte cell lines and primary cardiomyocytes reveals serious limitations and low resemblances to adult cardiac phenotype. *J Mol Cell Cardiol.* 2022 Apr;165:19–30.

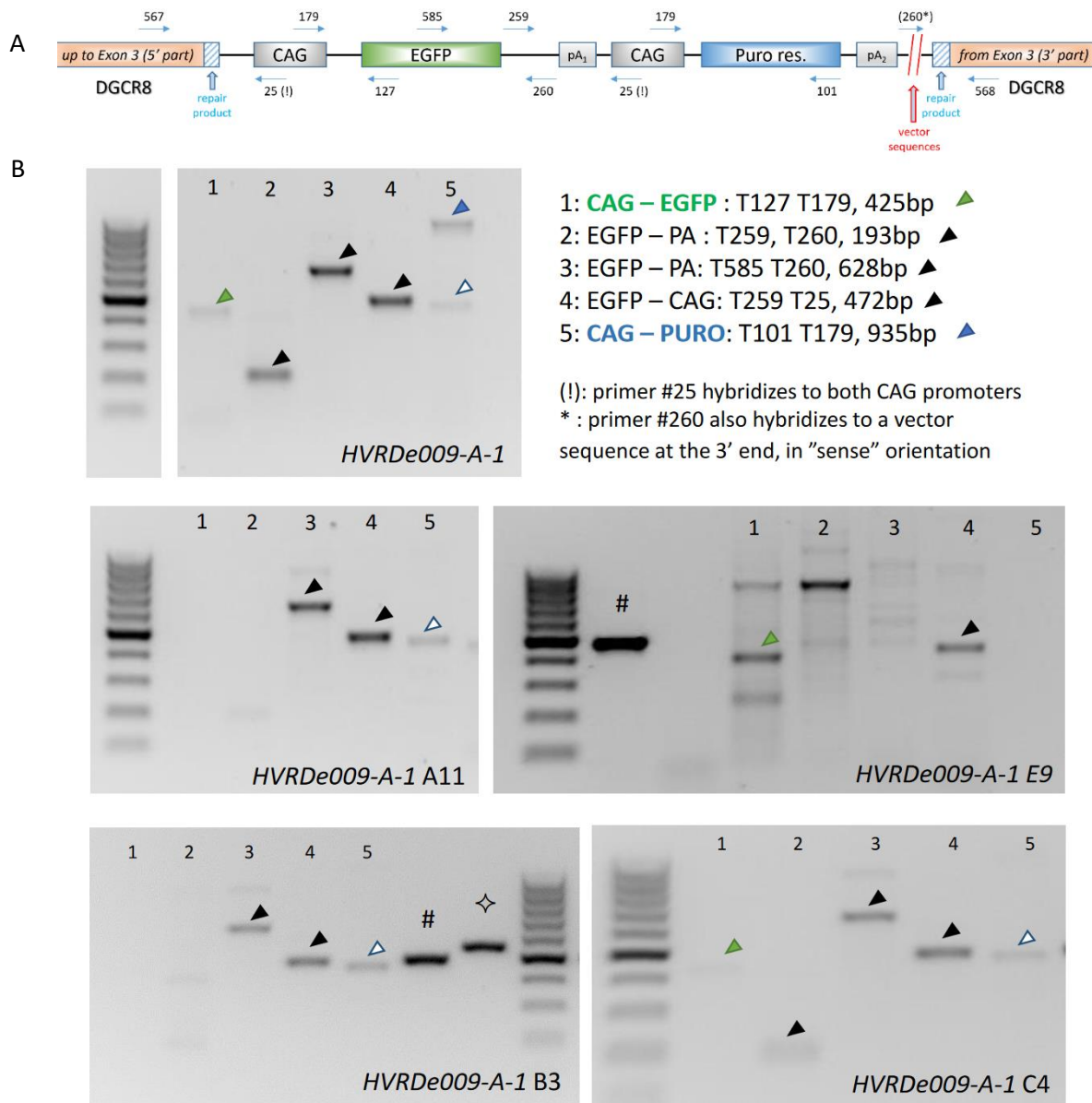
10. Acknowledgements

I would like to express my sincere gratitude to the individuals who have played a crucial role in the completion of my doctoral dissertation. First and foremost, I am immensely grateful to my supervisor, Dr. Ágota Apáti, for her invaluable guidance, continuous support, and patience throughout my Ph.D. study. Her expertise and mentorship have been instrumental in shaping the trajectory of my research. I would also like to extend my thanks to Dr. Nora Varga for her dedicated collaboration on the project, which has provided me with invaluable wet-lab and dry-lab experience. Her contributions have been essential in expanding my skill set and enhancing the overall quality of my work. Special appreciation goes to Adrienn Borsy for her assistance with conceptualization and molecular cloning for targeting CRISPR/Cas9. Her involvement has significantly contributed to the advancement of my research. I would like to acknowledge Dr. Tamás Orbán and his research group for their coordination of genotyping, miRNA, and Western blot assays. Their technical guidance and support have been instrumental in generating reliable data for my study. I am also grateful for the technical advice and assistance provided by Beáta Haraszi (Cell culture), Kornélia Némethy, László Homolya, Ábel Fóthi (Western blots, miRNA analysis), Orsolya Kolatsek (Western blots, GAGE PCR) and György Várady (Cell sorting). Their expertise has been invaluable in overcoming various technical challenges and ensuring the smooth execution of these experiments. Furthermore, I would like to express my appreciation for the support and collaboration of all my colleagues in the Pluripotent Stem Cell Laboratory. Their contributions have created a stimulating research environment and have been instrumental in my professional growth. I would like to acknowledge the insightful comments and suggestions provided by my institutional opponent, Antal Nyeste. His valuable input has greatly enriched the content and academic rigor of my thesis. To all the individuals mentioned above, I extend my sincere gratitude for your support and contributions. Your expertise and assistance have been indispensable in the successful completion of my doctoral dissertation.

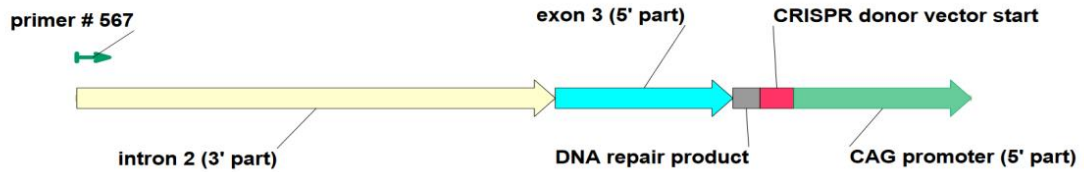
Supplementary material



Supplementary figure 1. Overview of the single cell cloning of GFP positive HVRDe009-A-1 without puromycin selection: GFP FACS analysis time points labeled green with the corresponding percentage of GFP expressing cells [206].



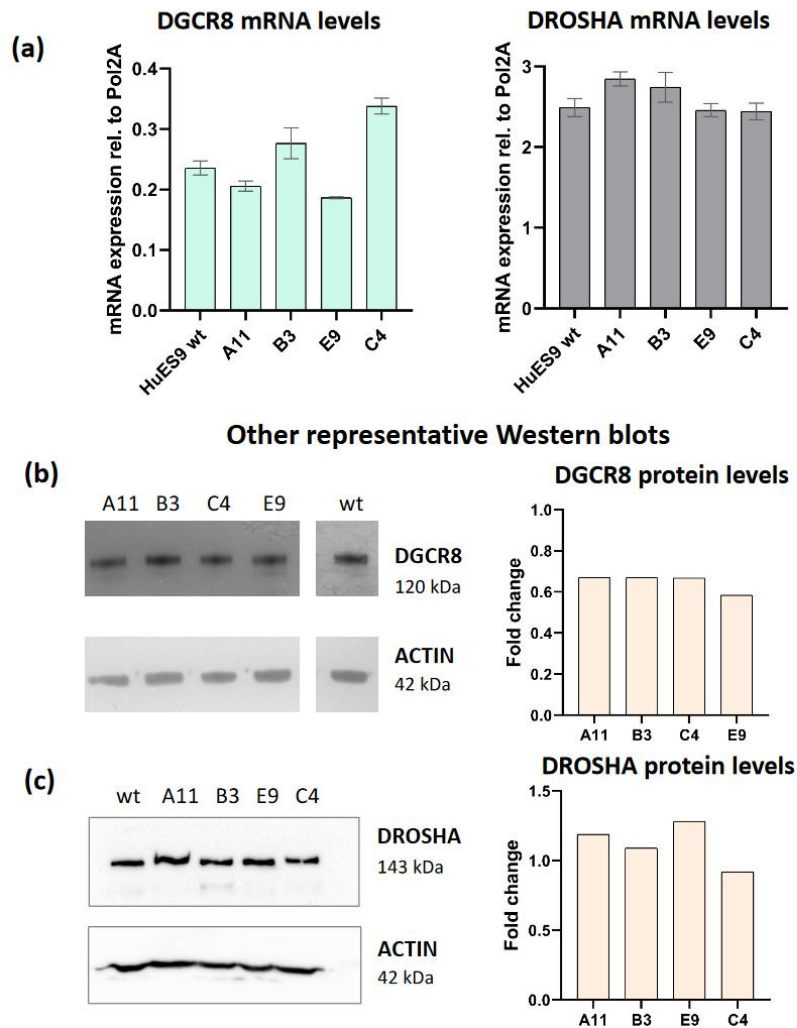
Supplementary figure 2. Diagnostic PCR results in the parental HVRDe009-A-1 cell line and the derived single cell clones: (A) Schematic overview of the targeting construct and primers (B) Diagnostic PCR results in the parental HVRDe009-A-1 cell line and the derived subclones. Each primer set covers a different fragment in the inserted cassette. Green, black, and blue arrows indicate the expected amplicon sizes. Empty arrows indicate unexpected amplicon sizes. #: amplifying the normal allele (with primers 567+568) [206].



	(361)	361	370	380	390	400
A11 clone (312)		ATATGGCGGAGACAGCGACCATCCGTCCTAATCGAATTCA				
B3 clone (312)		ATATGGCGGAGACAGCGACCATCCGTCCTAATCGAATTCA				
C4 clone (312)		ATATGGCGGAGACAGCGACCATCCGTCCTAATCGAATTCA				
E9 clone (312)		ATATGGCGGAGACAGCGACCATCCGTCCTAATCGAATTCA				
C5 clone transgene integration 5' end (361)		ATATGGCGGAGACAGCGACCATCCGTCCTAATCGAATTCA				
Consensus (361)		ATATGGCGGAGACAGCGACCATCCGTCCTAATCGAATTCA				
Section 11						
	(401)	401	410	420	430	440
A11 clone (352)		CTAGTCGAATTCAGTAGTGCGCGCGGCCGCTCTAGCCCCT				
B3 clone (352)		CTAGTCGAATTCAGTAGTGCGCGCGGCCGCTCTAGCCCCT				
C4 clone (352)		CTAGTCGAATTCAGTAGTGCGCGCGGCCGCTCTAGCCCCT				
E9 clone (352)		CTAGTCGAATTCAGTAGTGCGCGCGGCCGCTCTAGCCCCT				
C5 clone transgene integration 5' end (401)		CTAGTCGAATTCAGTAGTGCGCGCGGCCGCTCTAGCCCCT				
Consensus (401)		CTAGTCGAATTCAGTAGTGCGCGCGGCCGCTCTAGCCCCT				
Section 12						

Supplementary figure 3. Sanger sequencing of the selected HVRDe009-A-1 clones:

(A) Schematic representation of the 5' transgene sequence environment. The indicated primer was used for sequencing (B) Sanger sequencing of the DGCR8 allele in the HVRDe009-A-1-derived single cell clones. 5' residual sequence is labeled blue, NHEJ repair product is labeled grey, donor vector sequence is labeled with red and CAG promoter is labeled green. (For detailed sequence alignment see [206]).



Supplementary figure 4. Analysis of DGCR8 and DROSHA expression in the HVRDe009-A-1 clones: (A) Another biological replicate of relative mRNA expression levels; mean \pm SD values of technical replicates are shown. (B) A biological replicate of DGCR8 protein level measurement in the clones relative to the parental HuES9 (WT) cell line. (C) A biological replicate of Drosha protein level measurement in the clones relative to the parental HuES9 (WT) cell line. For (B) and (C), Western blot images are on the left, quantification results are on the right [206].